IEEE Access
Multidisciplinary | Rapid Review | Open Access Journal

Received January 23, 2018, accepted February 19, 2018, date of publication March 5, 2018, date of current version April 23, 2018.

Digital Object Identifier 10.1109/ACCESS.2018.2810855

Real Measurement Study for Rain Rate and Rain Attenuation Conducted Over 26 GHz Microwave 5G Link System in Malaysia

IBRAHEEM SHAYEA[1], THAREK ABD. RAHMAN[1], MARWAN HADRI AZMI[1], AND MD. RAFIQUL ISLAM[2]

[1]Wireless Communication Center, Universiti Teknologi Malaysia, Kuala Lumpur 54100, Malaysia
[2]Electrical and Computer Engineering Department, International Islamic University Malaysia, Kuala Lumpur 53100, Malaysia

Corresponding author: Ibraheem Shayea (ibr.shayea@gmail.com)

ABSTRACT In this paper, real measurements were conducted to investigate the impact of rain on the propagation of millimeter waves at 26 GHz. The measurements were accomplished using a microwave fifth generation radio link system with 1.3 km path length implemented at Universiti Teknologi Malaysia Johor Bahru, Malaysia. The implemented system consisted of Ericsson CN500 mini E-link, radio unit, rain gauge, and data logger. The measurements were attained and logged daily for a continuous year, with 1-min time intervals. Next, the MATLAB software was used to process and analyze the annual rain rate and rain attenuation, including for the worst month. From the analyzed results, it was found that at 0.01% percentage of time, the rain rate was 120 mm/hr; while the specific rain attenuation was 26.2 dB/km and the total rain attenuation over 1.3 km was 34 dB. In addition, the statistics acquired from the measurements for the worst month were lower than what was predicted by the international telecommunication union (ITU) model; around 51% and 34% for the rain rate and rain attenuation, respectively. The average percentage of error calculated between the measurements and predicted results for the rain rate and rain attenuation were 143% and 159%, respectively. Thus, it can be concluded that the statistics for the worst month in Malaysia is lower than what was predicted by the ITU model.

INDEX TERMS Millimeter wave, rain attenuation, propagation, microwave 5G link, access 5G link, tropical regions, fifth generation systems.

I. INTRODUCTION

Rain attenuation is one of the major obstacles facing the propagation of mm-waves in 5G systems [1]. The mm-wave signals can be absorbed, scattered, depolarized, and diffracted by rain. This can restrict their propagation, causing high signal attenuation loss through the effective propagation path length [2]–[5]. The impact becomes even more critical in tropical regions, like Malaysia, characterized by heavy and high rain rates with large raindrop sizes. The raindrop size distribution changes according to geographical location, and they can approach the size of radio mm-waves. This can strongly influence the propagation of mm-wave signals, causing high signal attenuation loss. The level of rain attenuation harshly increases when the rain rate, operating frequency, rain density, or the effective length are increased. This reduces the reliability, availability, and performance of the communication link. Thus, the spectrum becomes useless for mobile communications in 5G systems. To make matters worse, radio links in that range employ multiple-input and multiple-output (MIMO) techniques. Multifarious transmitting and receiving antennas are deployed to manipulate multipath propagation modes [6]–[10]. MIMO setups simultaneously send and receive numerous data signals on the same frequency channel. To enhance data rates, signals must be encoded in a way that exploits the independent fading and reflection of signals traveling through obstacles situated between the transmitter and the receiver. As such, high rain attenuation of the mm-wave band in tropical regions stand out as a key obstacle facing the implementation of 5G wireless system. Therefore, rain attenuation of mm-waves is a real and concerning issue which requires investigation, especially in tropical regions with consistent and heavy rainfall.

The high impact of rain on the propagation of electromagnetic waves had produced abundant studies which focused on

rain attenuation. These studies were conducted to investigate, and predict rain attenuation in different environments and over several frequency bands. The earliest confident measurement studies were conducted by Mueller [11], Robertson and King [12], Anderson *et al.* [13], and Wexler and Weinstein [14]. Consequently, numerous measurement studies were further conducted throughout the world. In Malaysia, the initial studies that had focused on rain attenuation over wireless communication systems were accomplished in the early 1990's at UTM [15] and at Universiti Sains Malaysia (USM) [16]. In these studies, real measurements were obtained from different locations and with various frequency bands. After 1997, more studies were carried out for different wireless systems and in various locations around Malaysia. Several scenarios with numerous system setups were considered in these studies, such as frequency characteristics [17], the frequency scaling method [18], path length reduction factor model [19]–[21], effect of wet antenna [22], raindrop size distribution [23], rain rate conversion [24], and performance of rain fade [20]. The effect of different frequency (F_c) bands in various locations [15], [17], [25], path lengths (PL) [26]–[28], rain rates (RR) [25], [29], and raindrop sizes [30]–[32] were investigated and discussed in several studies throughout the literature. The effect of polarization (PZ) types [33]–[38], horizontal polarization (HP) and vertical polarization (VP) were also investigated.

From the reviewed studies, it was observed that rainfall produces major attenuation to the propagated electromagnetic waves. The impact is more severe when the rain rate, operating frequency, or path length are increased [11]–[24]. It becomes critical with the horizontal polarization type, which produces more attenuation compared to vertical polarization. Although previous studies in the literature had provided a better understanding of wavelength behavior during a rainy environment, the candidate mm-wave bands for 5G systems and their signal propagation properties have not been properly characterized. This is particularly true for tropical regions, such as Malaysia, that are characterized by high rainfall intensity with the presence of large raindrops sizes compared to other regions. 26 GHz is one of the candidate frequency bands which has yet to be investigated and properly characterized for 5G systems. Most reviewed studies were conducted based on narrowband systems, while wideband systems that can carry higher data rate, up to 10 Gbps (as targeted in 5G systems), have not been properly investigated. Only a few studies [39]–[42] had focused on the wideband system; Hirata *et al.* [39] and [40] and Kallfass *et al.* [41]. However, these two studies were conducted for 120 GHz and 240 GHz, respectively, which are not from the 5G's candidate frequency bands (24 GHz to 86 GHz) [43]. Therefore, the candidate frequencies for the 5G system, such as 15 GHz, 23 GHz, 26 GHz, 28 GHz, and 38 GHz, require investigation. In addition, the annual rain statistics and worst month statistics should be thoroughly understood since these are essential information required for the design of the mm-wave wireless communication links for 5G systems, especially in tropical regions. It is necessary to have accurate information on rain attenuation statistics of the annual and worst months of the year. They are needed for predicting the appropriate rain attenuation margin and maximum rain attenuation levels of wireless communication links. Therefore, studies on the propagation of mm-waves during the event of rain are highly necessary in tropical regions, such as Malaysia. They will greatly contribute in characterizing and developing appropriate prediction models.

In this paper, real measurements were conducted to investigate the impact of rain on the propagation of mm-waves at 26 GHz. The measurements were carried out to understand the propagation behavior of 26 GHz link, and to pinpoint the rain attenuation margin level for this band at specific path lengths. The measurements were accomplished by using a microwave 5G radio link system implemented with 1.3 km path length at UTM Johor Bahru, Malaysia. The implemented system consists of Ericsson mini E-link model CN500, a radio unit, tipping bucket rain gauge model TB3, and data logger model DT80. The acquired measurements were continuously and daily logged in for one year, with one-minute time intervals. Consequently, the MATLAB software was used to annually process and analyze the rain rate and rain attenuation, including for the worst month. From the presented and discussed results, it was found that at 0.01%, the rain rate was 120 mm/hr, while the rain specific attenuation was 26.2 dB/km at 26 GHz frequency band. In addition, the worst month statistics from the real measurements for the rain rate and rain attenuation were lower than the predicted results from the ITU model by around 51% and 34%, respectively. The average percentages of error calculated between the measurement and predicted results for the rain rate and rain attenuation were 143% and 159%, respectively. It can be concluded that accurate annual and worst month statistics in Malaysia must be taken based on real measurement studies.

The rest of this paper focused on the following: the research background discussed in Section II. The rainfall in Malaysia, the impact of rainfall on the propagation of mm-waves, rain attenuation, and the worst month were all highlighted. Next, related measurement studies based on real measurements were presented and discussed in Section III. The experimental test bed and system equipment were then described in Section IV, followed by the numerical and measurement results and discussion in Sections V and VI, respectively. Finally, the conclusion of this paper was discussed in Section VII.

II. RESEARCH BACKGROUND

A. RAINFALL IN MALAYSIA

Rainfall characteristics in tropical regions significantly vary from temperate regions. In tropical regions, rainfall is normally high, with heavy thunderstorms and large raindrop sizes throughout the year [44]–[46]. Usually, rain has an average rainfall rate of at least 60 mm/hr worldwide [44]–[46]. Malaysia is one of the tropical regions characterized by a

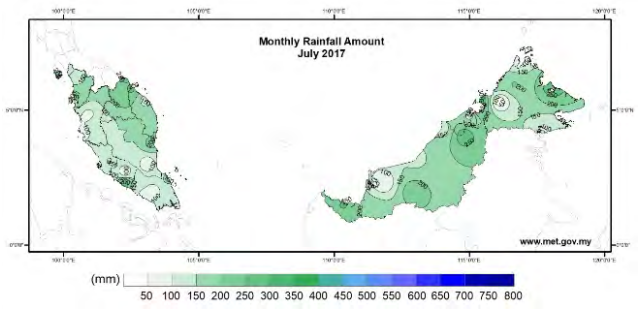

FIGURE 1. Monthly recorder rainfall in Malaysia [47].

high rainfall rate with large raindrop sizes and heavy rain; similar to other tropical regions. Figure 1 provides a summary of the rainfall rate recorded in Malaysia [47]. It shows that Malaysia has the highest amount of rainfall, which can exceed 200 mm/hr on average throughout the entire country [47], [48]. This rainfall is mostly very heavy with great amounts of lightning as opposed to temperate regions. Raindrop size also has a different characterization in tropical regions. Its distribution changes with geographical location and can be the same size of radio mm-waves. On the other hand, temperate regions are characterized by lower rainfall rate, milder rainfall intensity, and smaller raindrop sizes. They are normally identified by widespread precipitation which can cover larger areas, with lower rainfall rates that can reach around 25 mm/hr on average and throughout the year. The rain in temperate regions consist of small raindrop sizes with rain intervals that exceed one hour [49], [50].

In tropical regions, there are two climatic seasons: a dry season and a wet season. The dry season is characterized by lower rainfall rate with an average rainfall total of about 50 mm/hr [44], [51]–[53]. The wet season is categorized by a high rainfall rate. Equatorial climates also have the same characteristics as tropical regions in terms of their formation and raindrop sizes. They have the wet season throughout the year with average rainfall values of at least 60 mm/hr. The weather in such regions is hot and wet throughout all months of the year. Rainfall is also heavy and almost occur daily in the afternoon. Equatorial climates exhibit only very minor variations in temperature, both within a single day and throughout the year [44], [51]–[53].

B. IMPACT OF RAINFALL

Rainfall is a significant obstacle that hinders the propagation of mm-wave signals from the transmitter to the receiver. The signal can be absorbed, scattered, depolarized, and diffracted by raindrops [21], [25]–[29], [31], [33], [34], [39], [40], [54]–[93]; as illustrated in Figure 2. The interaction between incident electromagnetic radio waves and the rain-filled medium can restrict the propagation of mm-wave signals. This results in additional attenuation to the propagated signal. The influence of rain becomes more critical when the rainfall rate, the operating frequency band, or the effective path length further increase. Moreover, the impact of rain is significantly influenced by the polarization type. Figure 3 illustrates the influence of such factors that cause attenuation to the propagated signal.

The level of the rain rate has a significant effect for adding further attenuation to the propagated signal during a rainy period, as demonstrated in Figure 3 (a). The presented results confirmed that rain attenuation radically increases with the escalation of the rain rate; the increase of raindrop number. This is because such an increase will raise the interaction probability between the incident wave and the raindrops. Due to that interaction, the absorption, scattering, and diffraction of the propagated signals will further increase, as illustrated in Figure 2. This will cause significant attenuation to the propagated signal. Consequently, once the rain rate becomes higher, the communication link will be unreliable and unstable, or the connection may be lost altogether. That means the effect is more severe in tropical regions known for high rainfall rates and greater rainfall intensities.

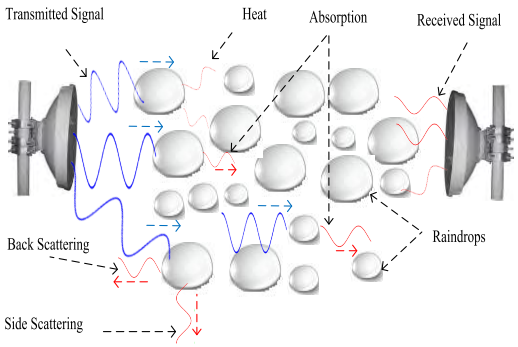

FIGURE 2. Impact of rain on the propagation of electromagnetic wave.

The impact of frequency bands is significant on the attenuation produced during the occurrence of rain, as illustrated in Figure 3 (b). The results indicate that rain attenuation becomes more critical with higher frequency bands. This is because the wavelength of higher frequency bands become smaller and approach the size of the raindrop. The Average Raindrop Size (ARS) or the average width (diameter) of the raindrop is around 1.67 mm [94]; while the wavelength of 10 to 100 GHz ranges between 30 mm to 3 mm. So, a significant interchange of energy will occur between the propagated mm-wave and the raindrops. Such an interaction will result in significant attenuation of the propagated signal. Thus, when the frequency bands become higher, the rain attenuation level of the propagated signal will increase.

The effective path length between the transmitter and receiver also affect the propagation of mm-waves during rainfall [96], [98]. Rainfall is not uniformly distributed along the radio path length. Therefore, the effective path length is not like the actual path length. It is calculated based on rainfall distribution. As a result, accurate rain attenuation is calculated as a function of the effective path length. When the effective path length increases, that means the rainfall

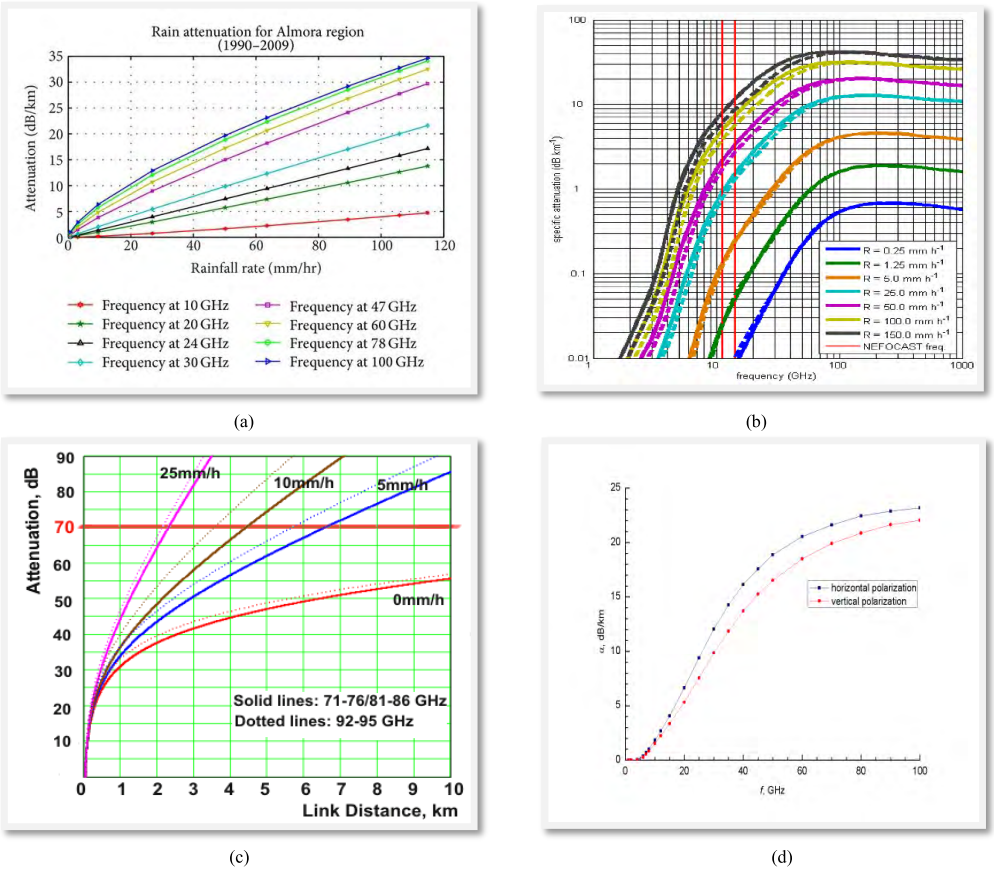

FIGURE 3. Rain attenuation with various rain rate, several frequency bands, various path length and different polarization types. (a) Rain attenuation versus rain rate [29]. (b) Rain attenuation versus frequency [95]. (c) Rain attenuation versus path length [96]. (d) Rain attenuation and polarization [97].

will cover a longer area between the transmitter and receiver which will produce further attenuation [36]; as illustrated in Figure 3 (c). Several research groups had investigated and proven this matter in their research, such as Alkholidi and Altowij [98], Abdulrahman *et al.* [26] and [27], and Korai *et al.* [28]. From their studies, it was noted that the total rain attenuation is directly proportional to the effective communication path length.

The polarization type also affects the propagation of electromagnetic waves. Several research groups had investigated the effect of horizontal and vertical polarizations, such as Shresthal and Choi1 [33], Thorvaldsen and Henne [34], Morita *et al.* [35], and Watson [36]–[38]. In Shresthal and Choi1 [33] study, with the same frequency band of 18 GHz, the same path length, the same rain rate, and utilizing the same system, the horizontal polarization resulted in 12.5 dB more than what had occurred in the vertical polarization. A similar conclusion was also obtained from Thorvaldsen and Henne [34] research. With the same frequency band of 26 GHz, the same path length, the same rain rate, and utilizing the same system, the horizontal polarization resulted in greater attenuation than what had occurred in the vertical polarization. From these studies, it was observed that the attenuation levels occurring from the horizontal polarization are significantly greater than those from the vertical polarization. The effect becomes more critical in heavy rainfall and higher frequency bands. Figure 3 (d) illustrates the impact of polarization on rain attenuation with various frequency bands. The horizontal polarization adds more attenuation compared to the vertical polarization, especially with higher rainfall rate and higher frequency bands.

Consequently, the high rain attenuation of the propagated electromagnetic waves due to the increase of rain rate, operating frequency band, effective path length, raindrop size, and polarization types will shorten the distance of the communication link or cause no communication link at all during rainfall when it comes to 5G systems. This effect becomes worse in tropical regions characterized by heavy rainfall, higher rain rate, and larger raindrop sizes. In other words, as rain attenuation further increases when the rain rate, operating frequency bands, and effective path length also increase, the coverage provided by the mm-waves of 5G systems will be very small compared to the cellular systems operating on frequency bands below 5 GHz. Thus, the disruption intervals and unreliable wireless communication will just increase throughout the day. This indicates that 5G systems would

require the setup of massive amounts of small base stations to cover the required area.

C. RAIN ATTENUATION

The total rain attenuation statistics [99], [100] was essentially calculated based on the amount of attenuation that occurs due to rain per unit distance. The amount of attenuation per unit distance is defined as Specific Rain Attenuation (SRA) measured in [dB/km]. The calculation of specific rain attenuation mainly depends on the rain rate level with the characteristics of rain and the incident electromagnetic waves at that specific location. The rain characteristics include the shape of the raindrops, rain orientation, rain temperature, and raindrop size distribution; while the characteristics of the electromagnetic waves include the frequency band, polarization type, and the direction of propagation at that point. The specific rain attenuation also depends on the forward scattering of the propagated electromagnetic wave. Its impact varies depending on the water temperature, the water refractive index, and the operating frequency bands. Therefore, part of the electromagnetic wave energy is absorbed by the raindrops and wasted as heat, while the rest is scattered in all directions [101], as illustrated in Figure 2. This scattered electromagnetic wave introduces undesirable or interfering signals into the desired received signal, which in turn, produces additional attenuation. Figure 2 illustrates the absorption and scattering of the radio wave when it incidents on a rain-filled medium. In case the wavelength of the propagated wave is short and approaches the raindrop size, the wave absorption becomes higher and the scattering becomes major. Consequently, the absorption and scattering of the electromagnetic wave mainly depends on the operating frequency, rain rate, raindrop shape, and raindrop size. Thus, estimating the specific rain attenuation mainly depends on the rain rate, frequency regression coefficients, and the polarization type. Accordingly, the specific rain attenuation is mathematically represented in Eq. 1:

$$\gamma = kR^{\alpha} \tag{1}$$

where k and α denote the regression factors that are subject to several factors such as drop size distributions (DSD), temperature, operating frequency, and radio wave polarization. The specific attenuation is also subject to the polarization type of the electromagnetic radiations due to the non-spherical nature of the raindrops. The attenuation level that results from vertical polarization waves is less than what can result from horizontal polarization [33]–[38]. The values of parameters k and α can be obtained from ITU Rec. P.838-3 [99].

The specific rain attenuation represented by Eq. 1 displays the rain attenuation per one km; while, the total rain attenuation's overall path length between the transmitter and receiver should be calculated by multiplying the specific rain attenuation, γ, with the actual path length, L, if rainfall is uniformly distributed. However, since rainfall is not usually uniformly distributed along the radio path length, calculating rain attenuation based on the actual path length will yield inaccurate results. Therefore, the horizontal homogeneity of rainfall must be considered. This phenomenon was identified as the effective path length of the communication link between the transmitter and receiver, which should be shorter than the actual radio path distance. It is utilized to evaluate the actual effective path length between the transmitter and receiver with a uniform distribution of rainfall. Based on that, the effective path length is introduced as another significant factor that should be considered in rain attenuation studies. To calculate the effective path length, L_{eff}, the distance reduction should be considered to estimate the actual path length with uniform rainfall distribution. Accordingly, a new matric was introduced and defined as the distance reduction factor "r", which is used for evaluating the effective path length between the transmitter and receiver. The mathematical evaluation for this matric is mainly subject to the actual path length, L, between the two communication sides and the assumption concerning the rain rate's structure of spatial distribution. Thus, the effective path length can be mathematically calculated in Eq. 2 [62], [83], [99], [102]:

$$L_{eff} = rL \quad (km) \tag{2}$$

where L_{eff} denotes the effective path length, r denotes the path reduction factor or distance factor as introduced by ITU [103], and L represents the actual path length of a link between the transmitter and receiver.

Several prediction models were suggested by different research groups to evaluate the rainfall horizontal variations in tropical regions [21], [104]. The most preferred and famous model applied in such regions would be the distance factor proposed by ITU [103]. The model is evaluated as a function of frequency, with rain rate at 0.01% percentage of time, exponent in the specific attenuation model, and actual path length. Although the ITU-R model can be employed to evaluate the rainfall horizontal variation, it is not the most optimum applicable model to be used in tropical regions. Therefore, several models were developed and proposed to evaluate the path reduction factor such as the revised Silva Mello model [58], the Abdulrahman model [20], and the Lin model [105]; all summarized in the following subsections.

1) ITU-R MODEL

The most confident and famous model employed for calculating the path reduction factor is the ITU-R Model [103], which is mathematically provided in Eq. 3:

$$r = \frac{1}{0.477 d^{0.633} R_{0.01}^{0.073\alpha} f^{0.123} - 10.579(1-\exp(-0.024L))} \tag{3}$$

where f denotes the frequency in GHz, $R_{0.01}$ is the rain rate at 0.01% percentage of time, α is the exponent in the specific attenuation model, and L is the actual path length between the transmitter and receiver. The maximum recommended value by ITU for "r" was 2.5; Eq. 3 was not used for small values for the denominator, providing larger values.

2) REVISED SILVA MELLO MODEL

The revised Silva Mello proposed a new model to estimate the path reduction factor values [58]. This proposed model is mathematically represented in Eq. 4:

$$r = \frac{1}{1 + \left[\frac{d}{d_0(R_p)}\right]} \tag{4}$$

where d denotes the actual distance between Tx and Rx, d_0 is the equivalent cell diameter given by $d_0 = 119R^{-0.224}$, and R_p is the rain rate at p percentage of time.

3) ABDULRAHMAN MODEL

Abdulrahman developed a model to evaluate the path reduction factor [20], as represented in Eq. 5:

$$r = \frac{1}{1 + \left[\frac{d}{2.6379(R_{0.01})^{0.21}}\right]} \tag{5}$$

where d denotes the actual distance between Tx and Rx, and $R_{0.01}$ is the rain rate at 0.01% percentage of time

4) LIN MODEL

Another path reduction factor model was developed by Lin [105]. This model is represented in Eq. 6:

$$r = \frac{1}{1 + \left[\frac{L}{L\,(R)}\right]} \tag{6}$$

where L denotes the actual path length between Tx and Rx, $L\,(R) = \frac{2636}{R-6.2}$, while R is the rain rate.

In all these models, the Complementary Cumulative Distribution Function (CCDF) of the rainfall rate and rain attenuation at one-minute rainfall rate is required. From the specific rain attenuation and the effective path length, the total rain attenuation over all effective path lengths exceeded for 0.01% of the time calculated, as introduced by ITU-R [103], [106]. Thus, from Eq. 1 and Eq. 2, the total rain attenuation over all effective path lengths that exceeded for 0.01% of time is given in Eq. 7:

$$A_{0.01} = kR^{\alpha} rL \tag{7}$$

where $A_{0.01}$ is the total attenuation in dB along all effective path lengths at 0.01% percentage of time.

The total rain attenuation at a different percentage of time (p) in the range of 0.001% to 1% can also be calculated based on ITU-R [103], [106] by utilizing the following mathematical expression:

$$A_p = A_{0.01} C_1 p^{-(C_2 + C_3 log_{10} p)} \tag{8}$$

with

$$C_1 = \left(0.07^{C_0}\right)\left\lfloor 0.12^{(1-C_0)}\right\rfloor rL \tag{9}$$

$$C_2 = 0.855C_0 + 0.546(1 - C_0) \tag{10}$$

$$C_3 = 0.139C_0 + 0.043(1 - C_0) \tag{11}$$

where

$$C_0 = \begin{cases} 0.12 + 0.4\left[log_{10}\,(f/10)^{0.8}\right] & f \geq 10\ GHz \\ 0.12 & f < 10\ GHz \end{cases} \tag{12}$$

D. WORST MONTH

Propagation conditions significantly vary between the months within a year. Moreover, the monthly changeability can noticeably vary from year to year. Therefore, it is impossible to know exactly what will happen in the next ten years as it may be more extreme than what is perceived so far. But, under the worst conditions, the propagation research groups can determine link availability and design a suitable link channel. To offer propagation data based on any month, it is essential to address this issue. Therefore, research groups established the idea of worst month; as introduced by the recommendation from ITU-R P.581-2 [107]. Thus, the worst month becomes a significant factor necessary for consideration to study rain attenuation in any communication system analysis. The worst month is known as a month in a period of twelve consecutive calendar months of the year in which rainfall exceeds the normal level for the longest time [107]. The worst month statistic can be obtained from real measurements continually conducted for one year or more. This is the most accurate way to guarantee that the characteristics of monthly variability are observed. However, in the case where the monthly statistics data are not accessible, the ITU model given in ITU-R P.841-5 [108] can be applied for obtaining the average yearly worst-month time percentage of excess, p_w, from the average yearly time percentage of excess, p, with the use of the conversion factor, Q. This is mathematically represented in Eq. 13:

$$p_w = Qp \tag{13}$$

where the value of Q ranges between 1 and 12, $1 \leq Q \leq 12$; while both p and pw denote the identical threshold levels. The parameter Q at p (%) is evaluated as a function of Q_1 and β. This is mathematically represented in Eq. 14:

$$Q_{(p)} = \begin{cases} 12 & for\ p < \left(\frac{Q1}{12}\right)^{\frac{1}{\beta}}\ \% \\ Q_1 p^{-\beta} & for\ \left(\frac{Q1}{12}\right)^{\frac{1}{\beta}} < p < 3\% \\ Q_1 3^{-\beta} & for\ \%3 < p < 30\% \\ Q_1 3^{-\beta}\left(\frac{p}{30}\right)^{\frac{\log\left(Q_1 3^{-\beta}\right)}{\log(0.3)}} & for\ p > 30\% \end{cases} \tag{14}$$

where the values of parameters Q_1 and β for various regions of the world are meticulously provided in Rec. ITU-R P.841-5 [108]. These two parameters of Q on p_w are simply derivatives from the above given dependence of Q on p. The resulting relationship for $12p_0 < p\,(\%) < Q_1 3^{(1-\beta)}$ is $\left(p_0 = \left(\frac{Q1}{12}\right)^{1/\beta}\right)$.

$$Q = Q_1^{1/(1-\beta)} p_w^{-\beta/(1-\beta)} \tag{15}$$

For global planning drives, ITU recommended suitable values for use; factor Q_1 should be 2.85 and β should be 0.13. Employing these parametric values led to the subsequent relationship between p and pw:

$$p\,(\%) = 0.30 p_w\,(\%)^{1.15} \quad for\ 1.9x10^{-4} < p\,(\%) < 7.8 \tag{16}$$

In Malaysia, the worst month statistics study was conducted at WCC, UTM, Johor Bahru, between the period of 1996 to 2000 [109], [110]. In that study, the rain rate was measured for three continuous years at three different locations. This study conducted real measurements for rain attenuation during several years at seven different locations in Malaysia. Two different frequencies bands were considered: 14.6 GHz band and 21.95 GHz. The study focused on measuring annual rain rate statistics and for the annual worst month based on real measurement data conducted in one year. The appropriate values for parameters Q_1 and β were obtained from the measured data utilizing the least squares method in Eq. 13. Table 1 presents the acquired values for these two parameters with the coefficient data. The presented values of Q_1 and β were estimated based on real measurement data continuously conducted for one year, while simultaneously considering the rain rate and rain attenuation [15]. The presented values in Table 1 emphasize that the relationship between the average annual and the average annual worst month are almost the same based on real measurement data for the rain rate or rain attenuation statistics. By taking the average values of Q_1 and β over both the rain attenuation and the rain rate statistics, the average value of Q_1 was "0.916" and β was "0.303". These average values can be the best recommended values for the Malaysian tropical climate.

TABLE 1. Predictable $Q1$ and β values based on one year real measured data [111].

Criteria	Q_1	β
Based on the Rain Rate	0.8913	0.29
Based on the Rain Attenuation (14.6 GHz)	0.9495	0.30
Based on the Rain Attenuation (21.9 GHz)	0.9078	0.32
Average	0.916	0.303

TABLE 2. $Q1$ and β values based on a real measurement and ITU-R model [112], [113].

Location	Q_1	β
UTM, Malaysia	0.92	0.30
USM, Malaysia	1.39	0.30
Average for Malaysia	1.155	0.3
Indonesia	1.70	0.22
ITU-R	2.85	0.13

The same values were also stated by other researchers in Malaysia and Indonesia [112], [113]; as illustrated in Table 2. The obtainable values of Q_1 and β parameters were presented based on measured data from various locations, as well as the predicted data by the ITU-R model. The presented results indicate that the obtainable Q_1 value from the measured data in Indonesia is much closer to the predicted value by the ITU-R, with a percentage of error around 40.4%. On the other hand, the obtainable β value from the measured data in USM, Malaysia seems to be the closest to the predicted β value by the ITU-R model, with a percentage of error around 53.8%. The presented data in Table 2 demonstrates that the predicted Q_1 and β values by the ITU-R model are not accurate as compared to the obtainable values from the measured data in Malaysia and Indonesia. As a result, the predicted Q_1 and β values of the ITU-R model are not consistently accurate values for all tropical regions. Thus, more accurate values for Q_1 and β can be obtained from real measurements.

III. RELATED MEASUREMENT STUDIES

Rain attenuation studies based on real measurements began early in the forties during the last century. In 1946, the propagation of 6-mm waves was conducted by Mueller at the Bell Telephone Laboratories in New York [11]. Real measurements were made to assess the rainfall attenuation at a wavelength of 0.62 centimeter (cm). From that study, it was found that moderate rain at 0.62-cm produced 0.6 dB/mile/mm/hr in a one-way connection. In the same year of 1946, another measurement study was accomplished by Robertson at Bell Telephone Laboratories in New York [12]. He studied the effect of rain on the propagation of 1.09 cm wavelength in the region between 1 cm and 4 cm. It was observed that more than 25 dB attenuations resulted per mile in rain of cloudburst proportions. In addition, the rain attenuation of waves longer than 3 cm in light and moderate rainfall was reduced, but may reach up to 5 dB per mile through the cloudburst. In 1947, another measurement study on rain attenuation of 1.25 cm was conducted by Anderson at the United States Navy Electronics Laboratory in California [13]. That experimental system setup contained an optical path length with 6400 feet and nine units of rain gauges placed in equal space. Both uniform and non-uniform rainfall rates were utilized in the experimental system. From that study, it was noticed that light to moderate rainfall may reduce the normal communication link without rainfall by about 10%. In 1948, another measurement study on rain attenuation due to rainfall intensities of centimeter electromagnetic waves was conducted by Wexler at Signal Corps Engineering Laboratories in Belmar, New Jersey [14]. These were the first positive real measurement studies conducted throughout the entire world. Since then, several measurement studies were accomplished in different environments worldwide. The effect of different frequency bands in various locations, path lengths, rain rates, raindrop sizes, rain temperatures, polarization, and other factors were investigated and discussed in numerous studies found in the literature. Table 3 provide a brief summary on various studies from the literature conducted in different regions throughout the world. The summary illustrates where the studies were conducted, the experiment system type, the operating

TABLE 3. Rain attenuation based on real measurement studies conducted over microwave link system at 0.01% percentage of time.

Author [Ref.]	Location	F_c [GHz]	MP	PZ	PL [km]	RR [mm/hr]	RA [dB]
Sujan [33]	South Korea	18	3 Ys	HP	3.2	50	33.38
				VP			21.88
Sujan [33, 69]	South Korea	38	3 Ys	VP	3.2	50	20.89
Akihiko [39]	Japan	120	20 Ms	VP	0.4	~ 60	62.5
Mauludiyanto [67]	Indonesia	28	15 Ds	-	0.056 4	-	~ 4 to ~ 36
Medeiros [59]	UK	36	12 Ms	-	4.1	12.5	14.8
Joerg [71]	USA	52	1 Y	VP	0.504	0.2 ~ 30	0.4 ~30
Joshi [56]	India	35	12 Ms	DP	0.230	~ 27.5	38
Korai [28]	Pakistan	28	3 Ms	-	0.2	~ 65	2.2
					0.4		4.44
					0.6		6.7
					0.8		8.8
					1.0		11

TABLE 4. Rain attenuation based on real measurement studies conducted in Malaysia at 0.01% percentage of time.

Location	System	F_c [GHz]	M. Period	PZ	PL [km]	RR [mm/hr]	RA [dB]
UTM-Skudai [26, 27]	MWL	14.8	1 year	HP	5.83	~130	~ 36 dB
UTM Kuala-Lumpur. [26, 27]	MWL	14.8	1 year	HP	3.96	~135	~ 31 dB
Penang [26, 27]	MWL	14.8	1 year	HP	11.3	~125	~ 43
Taiping [26, 27]	MWL	14.8	1 year	HP	3.48	~150	~ 30
Temerloh [26, 27]	MWL	14.8	1 year	HP	5.36	~120	~30
Alor Star [26, 27]	MWL	15.3	1 year	HP	4.85	~110	~ 29.5
Skudai, Johor Bahru, [70]	PTP link	23	13 months	-	1.3	60	15
						90	30

frequency (F_c) investigated, the Measurement Period (MP) of time (Year (Y), Month(M), and Day (D), the considered Polarization (PZ) type, whether it was a Horizontal Polarization (HP) or a Vertical Polarization (VP), the Path Length (PL) of the experimental setup between the transmitter and receiver, the measured rain rate, and the rain attenuation level discovered from each individual measurement study.

In Malaysia, several studies were conducted to investigate and predict the rain attenuation level in different locations and over various frequency bands. The first research studies that focused on rain attenuation over wireless communication systems were accomplished in the early 1990's at UTM [15] and at USM [16]. In these two studies, real measurements were acquired from diverse locations based on various frequency bands. Since then, rain attenuation studies have been massively conducted in different areas for various frequency bands, as illustrated in Table 4. After 1997, more rain attenuation studies were carried out in Malaysia for different wireless systems and in various locations. Most of these studies began by experimental set-up, followed by the collection of data and the analyzing of measurements collected from that data. Most of the conducted measurements from the collected data are within one-minute intervals. Next, the data were utilized for developing and proposing new prediction models to estimate rain attenuation statistics. The measurements accomplished in Malaysia were made for different system types, such as microwave line-of-sight (LOS) links, terrestrial links, and satellite links. Moreover, these studies considered several scenarios with various system set-ups, such as the frequency characteristics [17], the frequency scaling method [18], path length reduction factor model [19]–[21], effect of wet antenna [22], raindrop size distribution [23], rain rate conversion [24], and performance of rain fade [20]. These studies had contributed a better understanding of the behavior of the wavelength during a rainy environment, along with the rain attenuation level and rain fading margin in Malaysia. The measurement results were used to investigate prediction models from the literature to determine more accurate models that can be employed for predicting rain attenuation in Malaysia. Several new prediction models were developed to first predict the path reduction level, then the rain attenuation level in Malaysia based on the collected data from real measurements.

From these real measurement studies conducted in different environments, it was observed that rainfall produces significant additional attenuation for electromagnetic waves. The effect further increases with the increase of the rain rate, path length, or operating frequency band. In addition, the polarization type produces different attenuations; whereby, horizontal polarization adds more attenuation as compared to vertical polarization. The impact of horizontal polarization further increases with higher frequency bands and higher rain rate. This increase in rain attenuation impacts communication connectivity and system reliability. Besides the absorption of rain impact, the candidate mm-wave bands for 5G systems and their signal propagation properties have not been properly characterized. This is particularly true for tropical regions, like Malaysia, known for high rainfall intensity and large raindrop sizes in comparison to other regions. The 5th generation systems will utilize MIMO techniques to improve data rate and spectrum efficiency. To enhance data rates, signals must be encoded in a way that exploit the independent fading and reflection of signals traveling past obstacles located between the transmitter and receiver. Thus, basic knowledge of channel propagation characteristics of this new frequency band in tropical regions is important for the successful development of the 5G wireless system. Although there have been numerous studies conducted to examine the effect of rain on the propagation of mm-waves, there still remains insufficient propagation measurements and

a lack of channel modelling research for mm-waves; especially during rainfall in tropical regions.

Most of the previous studies were conducted based on narrowband systems, while the wideband systems that can carry higher data rate of up to 10 Gbps (as targeted in 5G systems) have not been properly investigated. Only a few studies had focused on the wideband system, such as the studies of Hirata *et al.* [39] and [40] and Kallfass *et al.* [41]. However, these studies were conducted based on very high frequency bands of 120 GHz and 240 GHz, respectively. These bands are not the candidate frequency bands for 5G systems, whereby the best candidate frequency bands are between 24 GHz to 86 GHz [43]. Therefore, the candidate frequencies for the wideband 5G systems such as 15 GHz, 23 GHz, 26 GHz, 28 GHz, and 38 GHz must be extensively investigated. In addition, the annual rain statistics and worst month statistics are necessary and essentially needed for the design of mm-wave wireless communication links for 5G systems. It is crucial to have accurate information on the rain attenuation statistics of the annual and worst months of the year. Such information is required for predicting appropriate rain attenuation margins and maximum rain attenuation levels of wireless communication links. Therefore, researching the propagation of mm-waves during the event of rain is highly needed in tropical regions such as Malaysia. This will greatly contribute to the characterization and development of appropriate prediction models.

IV. EXPERIMENTAL TEST BED AND SYSTEM EQUIPMENTS

Planning a wireless communication system that can achieve high performance throughout all months of the year is highly needed. Therefore, an experimental test bed was established to study the effect of rainfall on the propagation of mm-waves that will be used in 5G systems. The link was established between two LOS locations: WCC and Balai Cerapan at UTM, Skudai, Johor Baru. Figure 4 provides a description of the set-up locations and links based on Google maps. The link path between the transmitter and receiver was 1.3 km, while the operating frequency for both the transmitter and receiver was set to 26 GHz. Figures 5 and 6 provide a general description of the block diagram and the real set-up experiment

(a) (b)

FIGURE 4. Location of the path link from Google map [115]. (a) Top view. (b) Side view.

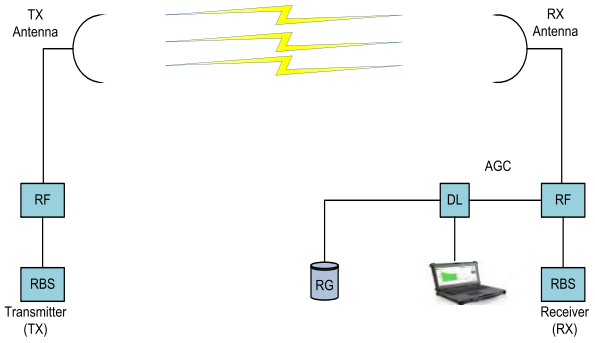

FIGURE 5. Block diagram of the experimental test bed system.

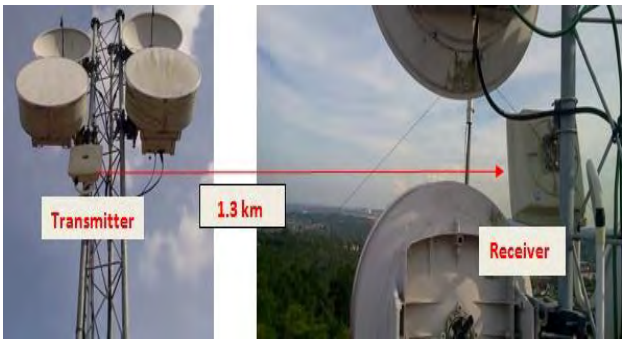

FIGURE 6. Actual experimental test bed system.

test bed system, respectively. As seen from the two figures, the system has two Radio Base Stations (RBSs) where each base station has one Radio Frequency (RF), antenna, and Automatic Gain Control (AGC). The system consists of one Data Logger (DL), Rain Gauge (RG), and one Personnel Computer (PC). These instruments were connected, as illustrated in Figure 6. Besides the hardware equipment, the MATLAB software was used to analyze the collected data from the measurements. Since the set-up path length is known for a specific link path length, the influence of Fresnel zone clearance was considered. The Fresnel zone points out the LOS clearance without any obstruction [114]. As indicated in the literature, when the first Fresnel zone is above the value of 0.6, the Fresnel zone is unrestricted by any obstacles [114]. In this system setup, the ATDI ICS Telecom software was employed to measure the Fresnel zone. The obtained Fresnel zone value was above 0.6 at the first Fresnel zone; as showed in Figure 7 [116]. Details of the system settings for the 26 GHz radio link are illustrated in Table 5. The main three equipment used in this experimental setup system included the radio transmitter and receiver units, Rain Gauge, and Data Logger; which are briefly described in the following subsections.

A. TRANSMITTER - RECEIVER RADIO UNIT

The Ericsson E - mini link CN 500 is the unit used as the Transmitter (TX)-Receiver (RX) component for the 26 GHz link. This radio unit is known for its high-performance

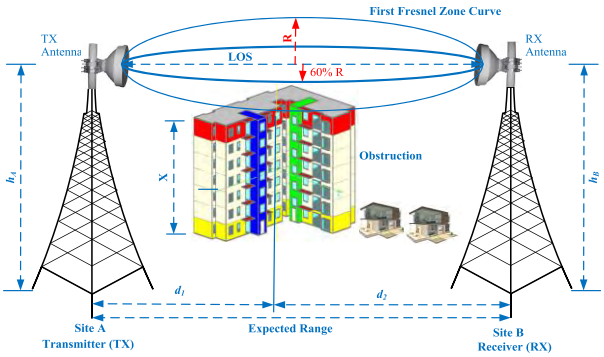

FIGURE 7. Fresnel zone clearance link.

TABLE 5. Communication system setting.

Parameters	Details
Standard of the system	IEEE 802.16
Operating frequency	26 GHz
System bandwidth	28 MHz
Number of channel	4 Channel
Modulation scheme	QPSK
Data rate	386 Mbps
Maximum Transmitted power	18 dBm
Sensitivity	- 84 dBm
Antenna Gain	41.0 dBi
Application	Board casting Mobile
Frequency Band Type	Licensed

radio link. It is classified as one of the best radio units that can produce longer hops of radio output power and with smaller antennas. This unit can be employed in various networks such as the mobile backhauls network, fixed broadband services over microwave link, national security, broadcasting, and enterprise. Figure 8 illustrates the physical structure of the Ericsson E - mini link CN 500 radio unit. It contains the radio unit, antenna set, and the modem unit, respectively. The collected data from these units are usually in automatic gain control (AGC) voltage. But in the analysis, they were converted to the dB power by utilizing a particular mathematical model given by the contractor, Ericsson. The mathematical model is represented in Eq. 17:

$$RF_{in} = 40\,(AGC\ level\ in\ volts) - 120 \qquad (17)$$

whereby, RF_{in} denotes the received signal in dBm, and 120 is the slope of conversion graph.

B. RAIN GAUGE

The rain gauge tipping model, TB3, is a small-sized equipment of 0.5 mm used to count and record the quantity of rainfall per minute. The rain gauge has 0.5 mm sensitivity and is configured to only record the rainfall data during the event of rain; while in the event of no rain, time is not recorded. Next, the recorded data are logged into the data logger every minute. Figure 9 shows the rain gauge set that was used in the system and the tipping bucket size.

C. DATA LOGGER

In this research, the data logger (also identified as the data taker model DT80), was used to record the rain rate and received signal strength. The physical photo of this device is presented in Figure 10. This device has analogue and digitals channels that also consist of counter, serial, and calculated channels. In addition, the data logger includes alarms, analogue sensors, TCP/IP services, scheduling of data acquisition, interfaces for communication, and physical system environment.

V. NUMERICAL RESULTS AND DISCUSSION

In this subsection, the influence of rain on the propagation of electromagnetic waves are investigated and examined. That were performed based on numerical results obtained theoretically from mathematical evaluations utilizing MATLAB software. The evaluations were performed based on the ITU models introduced in Rec. ITU-R P.530-16 [103] as well as the required parameter values in Rec. ITU-R P.838-3 [99]. These numerical results aim to illustrate the interaction between the incident electromagnetic radio waves and the rain-filled medium with various rain rates, several operating frequency bands, diverse path lengths, and different polarization types.

A. INFLUENCE OF RAINFALL RATE

The rain rate is considered as one of the major obstacles that restrict the propagation of electromagnetic waves in tropical regions. Usually, when the rainfall intensity increases, the rain attenuation of the mm-wave radically increases as well. Figure 11 illustrates the impact of the rain rate on specific rain attenuation [dB/km] with various frequency bands and two different polarization types. The graph confirmed that the impact of rainfall further increases when the rain rate increases. This is because when the rainfall intensity rises, the absorption, reflection, scattering, depolarization, and diffraction of the electromagnetic wave signals also increase. The results indicate that a rain rate of 10 mm/hr to 270 mm/hr with a horizontal polarization and frequency band of 30 GHz produce rain attenuation ranging between 1.96 to 56.8 dB/km. Meanwhile, a rain rate of 10 mm/hr to 270 mm/hr with a vertical polarization and frequency band of 30 GHz produce rain attenuation ranging between 1.7 to 45.1 dB/km. This very large attenuation indicates that the effect of rain on the propagation of mm-waves in tropical regions is very high. This causes unreliable communication, especially during heavy rainfall. For this reason, the propagation of mm-waves should be further investigated, and communication channels must be well designed for upcoming 5G systems.

B. INFLUENCE OF OPERATING FREQUENCY

The propagated electromagnetic wave is further attenuated when the operating frequency bands are increased; whereby, the rain attenuation is directly proportional to

FIGURE 8. Physical photo of the radio, antenna and modem units for the mini-link CN500.

(a) (b)

FIGURE 9. Physical photo of rain gauge set with tipping bucket size. (a) Rain gauge set with tipping bucket. (b) Rain gauge after setup.

FIGURE 10. Data logger (data taker model DT80).

the increase of operating frequency bands. The wavelength is mathematically evaluated by dividing the light speed $(3 \times 10^8\ m/s)$ with the frequency band. Consequently, in lower frequency bands, the wavelength becomes much greater than the average raindrop diameter; while in higher frequency bands, the wavelength approaches the average raindrop diameter. The size of the raindrop varies between 1 mm and 6 mm [117], while the average width (diameter) of the raindrop is around 1.67 mm [94]. Therefore, if the frequency band is 5 GHz, the wavelength will be equal to 60 mm, which is around 40 times greater than the average raindrop diameter. However, if the operating frequency is 26-GHz, the wavelength will be 11.5 mm.At this frequency band, the wavelength is only 6.9 times greater than the average raindrop size. Therefore, there will occur a significant interchange of energy between the propagated mm-wave and the raindrops. Such an interaction will result in major attenuation of the propagated signal. Thus, when the frequency band becomes higher, the wavelength will be smaller, and that will increase the interchange of energy that occurs between the propagated electromagnetic waves and the raindrops. This will increase the rain attenuation level of the propagated signal.

Figure 12 illustrates the rain attenuation level against the operating frequency bands. The results demonstrate that the rainfall rate of 130 mm/hr with horizontal polarization produces rain attenuation between 0.0055 to 30.2 dB/km when the operating frequency bands change between 1 GHz and 40 GHz. Meanwhile, the same rainfall rate with vertical polarization produces attenuation between 0.0035 to 25.76 dB/km when the operating frequency bands vary between 1 GHz and 40 GHz. It was observed that the increase in operating frequency bands led to higher rain attenuation. The effect becomes more critical with higher rain rates. Meanwhile, the rain attenuation in mm-wave bands between 10 GHz and 40 GHz are larger than what is experienced in conventional

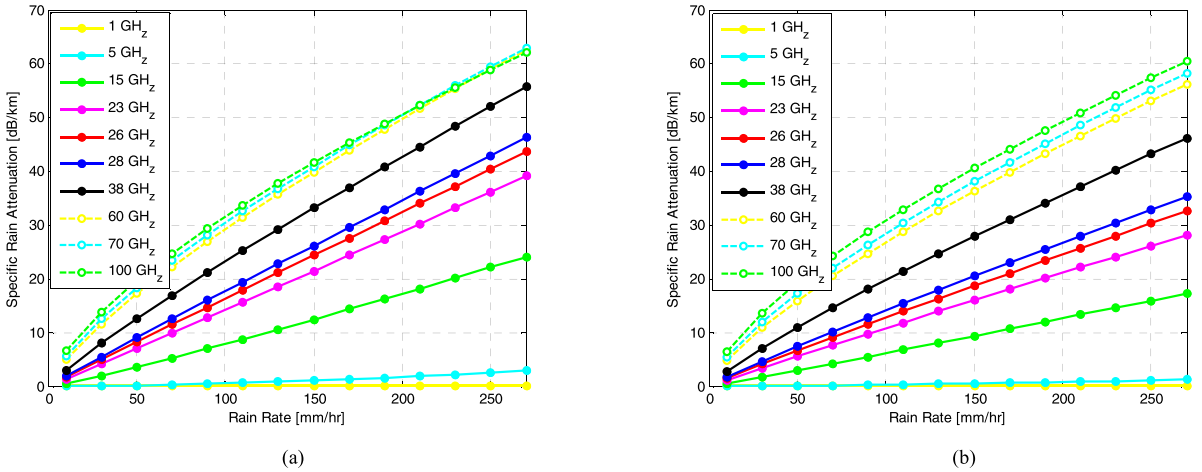

FIGURE 11. Impact of rain rate on the attenuation with different frequency bands and different polarization types. (a) Horizontal polarization. (b) Vertical polarization.

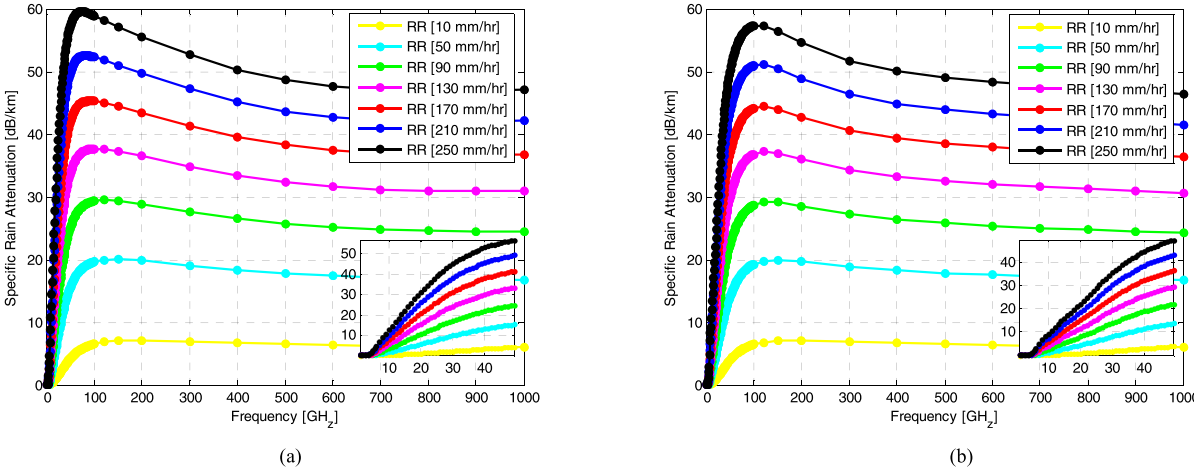

FIGURE 12. Impact of operating frequency on the attenuation with different frequency bands. (a) Horizontal polarization. (b) Vertical polarization.

systems below 10 GHz. This is because the wavelength of higher frequency bands become smaller and approach the usual raindrop size.

C. INFLUENCE OF EFFECTIVE PATH LENGTH

Besides the impact of the rain rate and operating frequency bands on the propagation of electromagnetic waves, the volume of rainfall also significantly contributes additional attenuation to the propagated signal. The actual volume of rain is measured by the effective path length, which is the actual path length of rain between the transmitter and receiver. This means that when the effective path length becomes longer, the covered rainy area between the transmitter and receiver becomes wider. Usually, rainfall is not uniformly distributed along the radio path length. Therefore, the effective path length is not similar to the actual path length; it is calculated based on the rainfall distribution. As a result, accurate rain attenuation is calculated as a function of the effective path length. Rain attenuation is directly proportional to the effective path length. Figure 13 clearly illustrates the impact of path length with various rain rates, several frequency bands, and different polarization types. The results emphasize that when the path length increases, rain attenuation further increases. This highlights the direct proportion between rain attenuation and effective length of the communication link. This means that mm-wave systems will have very small coverage and the communication length will further reduce during rainfall; especially if rainfall is heavy. Therefore, the path length between the transmitter and receiver should be properly designed when planning 5G channel systems to reduce the effect of rain on the propagation of mm-waves.

D. INFLUENCE OF POLARIZATION TYPE

Another factor affecting the propagation of electromagnetic wave is the polarization type. The effect of horizontal and vertical polarizations have been investigated by Shresthal and Choi1 [33], Per Thorvaldsen and Henne [34], Morita *et al.* [35], and Watson [36]–[38]. From these studies, it was noted that attenuation levels resulting from horizontal

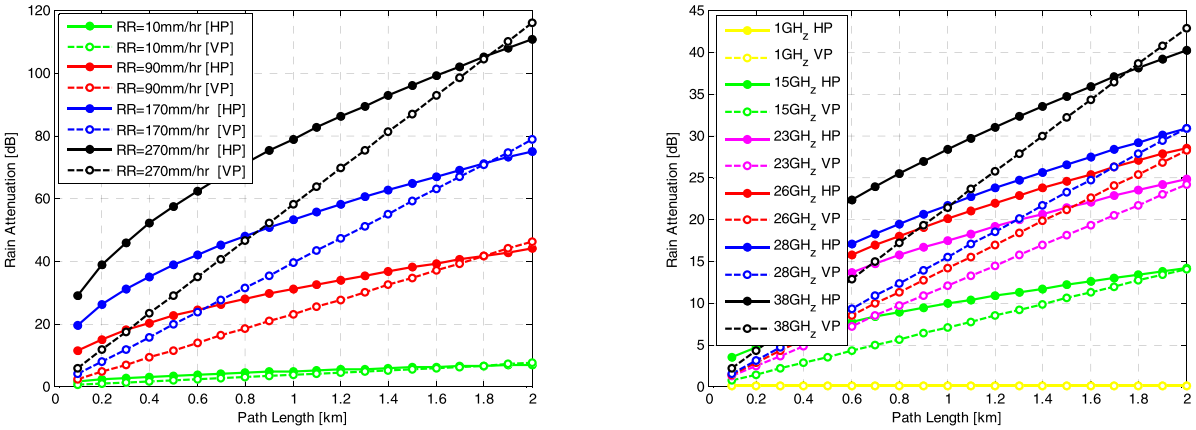

FIGURE 13. Influence of effective length on the rain attenuation. (a) Effect of rain rate [$f_c = 40GHz$]. (b) Effect of frequency [$RR = 90\ mm/hr$].

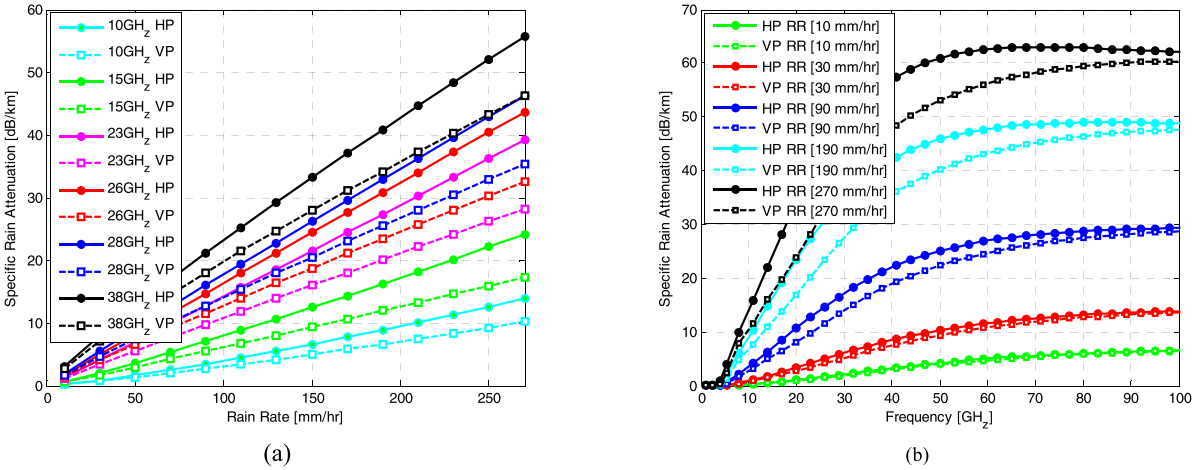

FIGURE 14. Impact of polarization on rain attenuation with various rain rate and different frequency bands. (a) Polarization with various RR. (b) Polarization with various frequency.

polarization are significantly greater than what results from vertical polarization. The effect becomes more critical during heavy rainfall and higher frequency bands. In this subsection, the impact of horizontal and vertical polarizations are theoretically investigated by utilizing the ITU-R P.530-16 [103] Model. Figure 14 illustrates the impact of different polarization types on rain attenuation with various rain rates and frequency bands. The results clearly indicate the differences obtained concerning rain attenuation from horizontal and vertical polarizations. Horizontal polarization always produces further attenuation as compared to vertical polarization. The same indication was observed with all rain rates and operating frequency bands. The difference becomes clearer when the rain rate or operating frequency bands are further increased. Consequently, it was noted that the horizontal polarization adds more attenuation compared to vertical polarization, especially with higher rainfall rate and higher frequency bands.

From these investigations, it was noted that the effect of rainfall further increases with the increase in rain rate, operating frequency, effective path length, and horizontal polarization. This effect increases disruption intervals, as well as unreliable wireless communication during a rainy period. That, in turn, decreases the communication reliability and stability. This radical increase in rain propagation loss will shorten the distance of the communication link, or no communication at all, during rainfall when it comes to 5G systems. This signifies that 5G systems would require the setup of massive amounts of small base stations to cover the required area.

VI. MEASUREMENT RESULTS AND DISCUSSION

In this section, the rain rate and rain attenuation statistics are analyzed based on the data collected by WCC's propagation research team from real measurements conducted in different locations throughout Malaysia for several years. The system daily recorded the data during the occurrence of rain for each minute, while non-rainy events were not recorded. The data were then logged every minute via the data logger. The mitigation frequency diversity technique with the switching

method was employed to solve link reliability during heavy rain. The collected data were then analyzed by applying the MATLAB software. Subsequently, the daily recorded data for every month were individually converted to CCDF at time, then the Monthly CCDF data were converted to annual CCDF at percentage of time. The CCDF data conversion from daily to monthly and then from monthly to annually were performed by utilizing the MATLAB software. Based on the analyzed data, this section presents and discusses the rain rate distribution, rain attenuation distribution, and worst month statistics.

A. RAIN RATE DISTRIBUTION

Malaysia is placed in the equatorial region, bounded by wide quantities of water from all directions. It is also characterized by intensive rainfall with high rain rates throughout the entire year. The distribution of rainfall mainly depends on the monsoon seasons, which are the Northeast and Southwest monsoons. The Northeast monsoon occurs between October and March, while the Southwest monsoon occurs between April and September. In addition, the rainfall in equatorial and tropical regions are categorized into three different types: drizzle, shower, and thunderstorm rainfalls; as illustrated in Table 6 [118]. In Malaysia, the most common rainfall that occurs would be the thunderstorm type. Based on previous studies conducted in Malaysia by our research center's team [15], it was observed that higher monthly rainfall rates occur in two seasons. The first season is between March and May, while the second season is between October and December of the year. However, it was simultaneously noted that in Malaysia, intense and heavy rainfall also occur and becomes distributed almost throughout the twelve calendar months of the year. From the measurements conducted in the specified three years, it was noticed that intense and heavy rainfall usually happen between 1.00 pm and 7.00 pm during the day; almost around 70%. Most of the time, the rain rate is always higher than 165 mm/hr, 101 mm/hr, and 50 mm/hr which takes place during an identical period (between 1.00 pm to 7.00 pm), with a percentage availability of 79%, 85%, and 96.8%, correspondingly. In this daily time (between 1.00 pm to 7.00 pm), rain intensities further vary between the hours. For example, the worst hours of rain intensities above 49 mm/hr and 81 mm/hr occur in the period between 1.00 pm to 2.00 pm, and from 2.00 pm to 3.00 pm during the day, respectively. As for the worst hours of rain intensities above 101 mm/hr and 165 mm/hr, they occur in the period between 3.00 pm to 4.00 pm, and from 5.00 pm to 6.00 pm during the day, respectively [15].

TABLE 6. Type of rainfall categorize.

Benchmark	Rainfall Type		
	Drizzle Rainfall	Showers Rainfall	Thunderstorm Rainfall
Rainfall rate	< 20 mm/hr	20 mm/hr – 70 mm/hr	70 mm/hr - 280 mm/hr
Rain Period	> 20 min	10 min - 25 min	4 min - 7 min
Nature (Happenings)	Slow and lengthy	Intermediate, without noise and lightning	Sudden with noise and strong lightning
Rain Cell Length [km]	> 15	4 - 15	< 3

According to the real measurements data conducted by WCC within several years in Peninsular Malaysia. Reference [15], the ITU-R model of rain rate distribution was examined based on one-minute rainfall data. According to the classification conducted by ITU-R, the region of Malaysia was classified as a climate in rain zone P. However, regarding the real measurements conducted within four years, from 1996 until 1999, it was found that Malaysia's rainy weather was categorized as falling between zone N and zone P, as illustrated in Figure 15. The presented results portray the cumulative distribution of rain intensity measured at different locations throughout Malaysia. From the conducted measurements for all locations, the collected data from the real measurements (for $P > 0.01\%$) was so close (most of the time) to what was predicted by ITU-R for zone P. There were a few differences between the measurement and predicted data by ITU-R, especially at lower percentages of time ($P < 0.01\%$) for all considered locations. For example, at 0.001% percentage of time, there was no average measurement value that reached 200 mm/hr; however, the predicted value by ITU-R for zone P was 250 mm/hr. Moreover, the measured rain rate of less than 0.05% percentage of time for all considered locations was much higher than what was predicted by ITU-R for zones N and Q. The measurement data at 0.001% percentage of time was closer to the predicted value by ITU-R for zone N. Even though there were a few differences between the measurements and the predicted data by ITU-R, the measured rain rate data confirmed that the results for various locations and during several years with one-minute rainfall rate illustrate that Malaysia has a rain climate that falls between the ITU-R rain zones N and P. The average rain rate at 0.01% percentage of time for all measured locations was 131.2 mm.

From the real measurement data conducted by WCC from June 2011 to May 2012 at UTM Johor Bahru, Malaysia, the CCDF rain rate is presented in Figure 16. Figure 16 (a) displays the monthly CCDF rain rate; while Figure 16 (b) presents the average CCDF rain rate throughout all months of the year. The presented results indicate that the monthly rain rate varies between 58 mm/hr to 136 mm/hr at 0.01% of time; while the average annual rain rate reaches 120 mm/hr. The results also demonstrated that the most rainfall throughout the year occurs in January. It was the worst month as compared to all other months. In addition, it was noted that the probability of rainfall rate rises when the time percentage level further decreases. This means that the link unavailability interval becomes shorter once the rain rate increases. For example, at 0.01% of time, the average CCDF recorded rain rate was 120 mm/hr, but once the time percentage became 0.001%, the rain rate increased to 168 mm/hr. However, the rain rate at 0.01% percentage of time was the considered rate in the entire statistical analysis. Rain rate at 0.01%

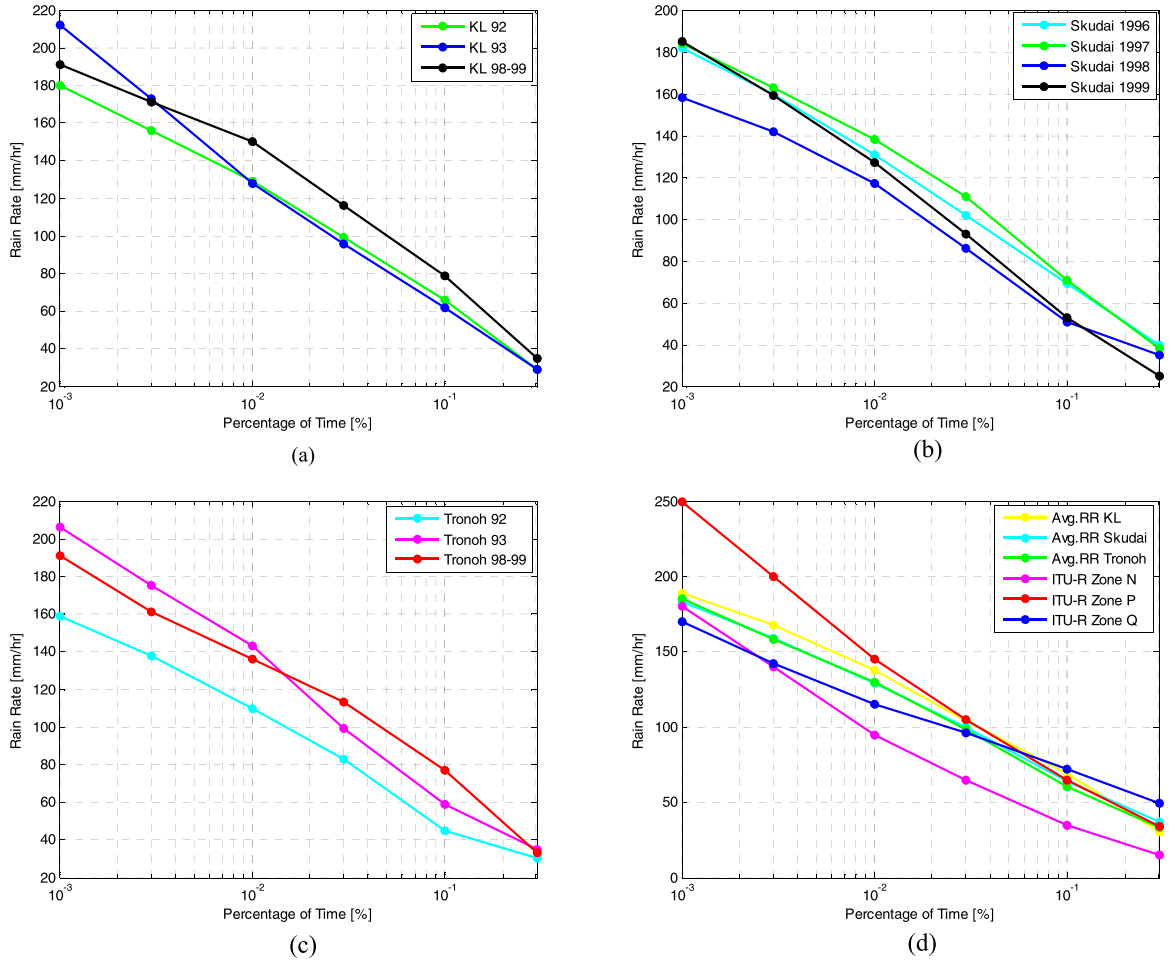

FIGURE 15. Cumulative distribution of rain rate based on measurement data conducted at three different places in Malaysia with various rain climate zones based on ITU-R model [15]. (b) Kuala Lumpur. (b) Skudai, Johor Bahru. (c) Tronoh area. (d) Avg. measurement and predicated data.

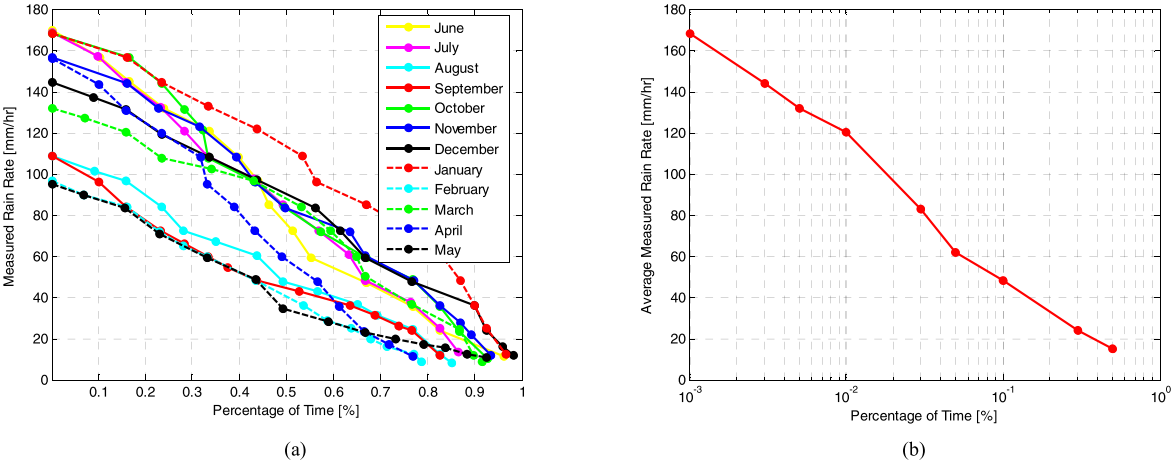

FIGURE 16. CCDF measured rain rate in Malaysia [June 2011 - to - May 2012]. (a) Monthly measured data. (b) Average overall months.

percentage of time is a very significant factor used to compute the rain attenuation [in dB] for a link at specific locations. Based on the presented and discussed results from the real measurements acquired during several years, it can be seen that from the previous research [15] conducted in the same location at UTM back in 1996-1999, the recorded rain

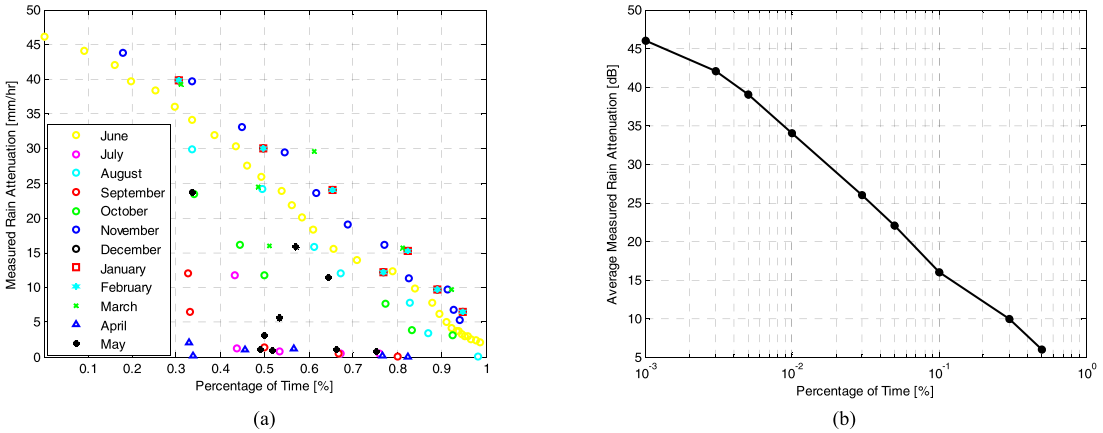

FIGURE 17. CCDF rain attenuation in Malaysia at 26 GHz. (a) Monthly record. (b) Average overall months.

rate at 0.01% percentage of time ($R_{0.01}$) was 125 mm/hr. From the CCDF data presented in Figures 15 and 16 at 0.01% of time, it was observed that the measured rain rate was almost similar at the UTM location in the year 2000 (120 mm/hr) and 2012 (125 mm/hr). Referring to the latest ITU-R P837 [58] proposed rain rate, the $R_{0.01}$ for Malaysia's region was 100 mm/hr. This will be an interesting aspect to analyze in future.

B. RAIN ATTENUATION DISTRIBUTION

Like the rain rate distribution, the rain attenuation was recorded for the radio link of 26 GHz, with 1.3 km as the path length between the transmitter and receiver. The data were collected by employing the data taker model DT80. The measurement data were daily recorded throughout all months of one continuous year, with 95% link validity at all times. The measurement with fade period was daily conducted and recorded during rain occurrence. From the daily recorder data for one month, the CCDF was converted to percentage of time (p%). Subsequently, the Monthly CCDF rain attenuation data were converted to the annual CCDF rain attenuation data at percentage of time (p%). The conversion from daily to monthly and from monthly to annual CCDF data, as well as the analysis of the original CCDF data, were achieved by utilizing the MATLAB software. Figure 17 (a) presents the - monthly CCDF of rain attenuation measured from June 2011 to May 2012, while Figure 17 (b) displays the CCDF for the average rain attenuation throughout all considered months. From the presented results, it was noted that the rain attenuation at 26 GHz is critical and resulted around 26.3 dB/km as specific rain attenuation at 0.01% percentage of time. That amount of attenuation can significantly degrade the communication link during rainfall. As a result, utilizing 26 GHz in tropical regions can only support short path lengths. In the case where operators would like to use it for a longer path length, the transmitted power and antenna gain must be increased to cover the targeted area.

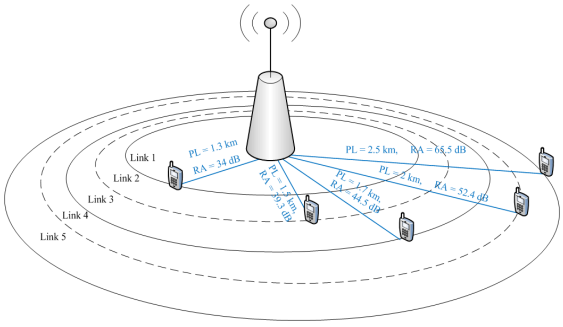

FIGURE 18. Estimated rain attenuation based on a real measurement recorded data.

Thus, rain attenuation will further increase in the event of rain if the effective path length becomes longer, as illustrated in Figures 13 and 18.

C. WORST MONTH STATISTICS

The rainfall rate in the worst month becomes more than usual as compared to other months throughout the year. The worst month is defined as the highest rain rate, rain attenuation, or other measurement parameters for that specific percentage of time based on the monthly CCDF data. Studying such statistics will boost a deeper understanding of rain attenuation of mm-waves during the worst month. This will contribute to the designing of an accurate and reliable communication link specifically suited for the worst month in new and upcoming 5G systems. Thus, the worst month statistical analysis is considered as a significant tool that should be employed for creating the wireless channel in 5G communication systems. The statistics for the worst month, such as the rain rate and rain attenuation, can be estimated by applying ITU-R recommendation models [107], [119]. In this subsection, the rain rate and rain attenuation are examined in the worst month based on real measurement data recorded in Malaysia.

TABLE 7. Worst month and annual statistic of rain rate at 0.01 % percentage of time.

RR [mm/hr]	Measured Annual RR	Annual Worst Month		ITU-R Prediction Error	ITU-R Prediction Error (%)
		Measured	Predicted by ITU-R		
0	0.9	1	2.6	1.6000	160%
20	0.7	0.8	2.089	1.2890	161%
40	0.6	0.7	1.827	1.1270	161%
60	0.2	0.3	0.703	0.4030	134%
80	0.055	0.15	0.229	0.0790	53%
100	0.030	0.07	0.135	0.0650	93%
120	0.011	0.035	0.056	0.0210	60%
140	0.004	0.015	0.023	0.0080	53%
160	0.0015	0.0023	0.010	0.0077	335%

TABLE 8. Worst month and annual statistics of rain attenuation at 0.01% of time.

RA [dB]	Measured Annual RA	Worst Month		ITU-R Prediction Error	% of ITU-R Prediction Error
		Measured	Predicted (ITU-R)		
0	0.89	1.1	2.6	1.5	136%
5	0.4	0.7	1.284	0.584	83%
10	0.3	0.4	0.999	0.599	150%
15	0.15	0.2	0.547	0.347	174%
20	0.06	0.1	0.247	0.147	147%
25	0.04	0.07	0.173	0.103	147%
30	0.018	0.04	0.087	0.047	118%
35	0.010	0.02	0.052	0.032	160%
40	0.0045	0.015	0.026	0.011	73%
45	0.0015	0.002	0.01	0.008	400%

1) RAIN RATE IN THE WORST MONTH

The rain rate during the worst month was analyzed and discussed based on the recorded rainfall data for one continuous year, with 95% link availability for all recorded time from the real measurements. Table 7 provides a summary of the measured annual and worst month rain rate statistics, which were then compared to the predicted rain rate for the worst month by the ITU-R model. The presented results illustrate the level and percentage of error that emerged from the ITU-R prediction model as compared to the real measurement data conducted in Malaysia. Figure 19 displays the CCDF rain rate probability for the measured annual data, measured worst month, and the worst month predicted by the ITU-R model. The predicted CCDF rain rate by the ITU model was based on the formula given in Rec. ITU-R P.841-4 [108]. From the acquired data in Table 7 and Figure 19, the measured rain rate in the worst month is noticeably greater than the measured annual rain rate. This emphasizes that the level of the worst month is higher than what happens in normal months throughout the year. The predicted results by the ITU model did highlight that; however, its predicted rain rate in the worst month was significantly greater than the measured annual and worst month data at all percentages of time. This indicates that the predicted results by ITU are not applicable for use to estimate accurate worst month statistics in Malaysia; whereas, the analysis data based on the recorded data provides more accurate results which can be used for designing the most optimal mm-wave channel in 5G systems.

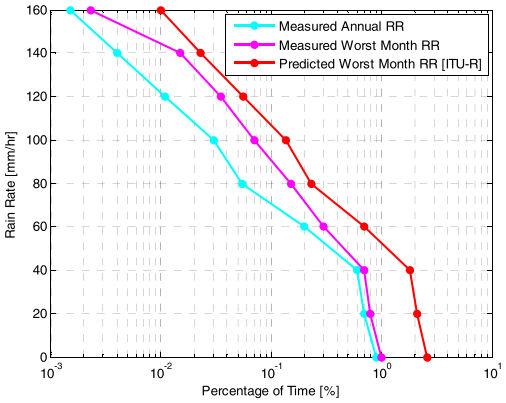

FIGURE 19. CCDF of the annual worst month rain rate at 0.01% percentage of time [June 2011 – May 2012].

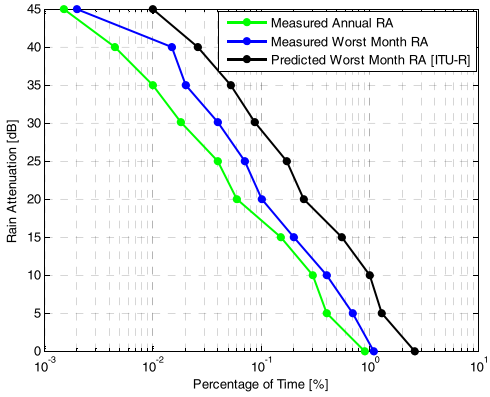

FIGURE 20. CCDF rain attenuation statistic for annual, measured and ITU-R predicted for the worst month.

2) RAIN ATTENUATION IN THE WORST MONTH

Besides the rain rate analyses, the rain attenuation in the worst month was also examined and discussed in this subsection. For the worst month, the rain rate further increases as compared to all other months. Rain attenuation becomes more critical in the corresponding month. Therefore, for the worst month, rain attenuation was analyzed and discussed based on real measurements data. Table 8 provides a summary of the measured annual and worst month rain attenuation statistics, which were then compared to the predicted attenuation during the worst month by the ITU-R model. The table also presents the level and percentage of prediction error by the ITU model. Figure 20 exhibits the CCDF rain attenuation probability for the measured data throughout the year, the measured worst month data, and the worst month predicted data by the ITU-R model. The presented results indicate that the measured rain attenuation data in the worst month is greater than the average measured annual rain attenuation data at all percentages of time. However, the predicted rain attenuation by the ITU-R

model for the worst month was significantly greater than the measured annual and worst month data for all percentages of time. This indicates that the predicted results by ITU are not applicable for use to design an accurate estimation channel in 5G systems. It can be used to provide an indication about the worst month statistic, but the results are not highly accurate in comparison to what was obtained from the real measurements.

VII. CONCLUSION

In this paper, the rain rate and rain attenuation of 26 GHz frequency band link were assessed and discussed based on real measurements conducted over microwave 5G radio link systems in Malaysia. From the presented and examined results, it was found that at 0.01%, the rain rate was 120 mm/hr, the specific rain attenuation was 26.2 dB/km, and the total rain attenuation over 1.3 km was 34 dB. Furthermore, the worst month statistic obtained from the real measurements was lower than what was predicted by the ITU model; around 51% and 34% for the rain rate and rain attenuation, respectively. The average percentage of error calculated between the measurement and predicted results for the rain rate and rain attenuation was 143% and 159%, respectively. Thus, it was concluded that the worst month statistic in Malaysia is lower than what was predicted by the ITU model.

REFERENCES

[1] T. S. Rappaport *et al.*, "Millimeter wave mobile communications for 5G cellular: It will work!" *IEEE Access*, vol. 1, pp. 335–349, May 2013.

[2] Z. Yun and M. F. Iskander, "Ray tracing for radio propagation modeling: Principles and applications," *IEEE Access*, vol. 3, pp. 1089–1100, 2015.

[3] X. Yin, C. Ling, and M.-D. Kim, "Experimental multipath-cluster characteristics of 28-GHz propagation channel," *IEEE Access*, vol. 3, pp. 3138–3150, 2015.

[4] J. C. Aviles and A. Kouki, "Exploiting site-specific propagation characteristics in directional search at 28 GHz," *IEEE Access*, vol. 4, pp. 3894–3906, 2016.

[5] X. Yin, Y. Ji, and H. Yan, "Measurement-based characterization of 15 GHz propagation channels in a laboratory environment," *IEEE Access*, vol. 5, pp. 1428–1438, 2017.

[6] X. Li, X. Yang, L. Li, J. Jin, N. Zhao, and C. Zhang, "Performance analysis of distributed MIMO with ZF receivers over semi-correlated $\mathcal{K}$ fading channels," *IEEE Access*, vol. 5, pp. 9291–9303, 2017.

[7] L. Liu, D. W. Matolak, C. Tao, and Y. Li, "Analysis of an upper bound on the effects of large scale attenuation on uplink transmission performance for massive MIMO systems," *IEEE Access*, vol. 5, pp. 4285–4297, 2017.

[8] C. Sanchis, M.-T. Martínez-Ingles, J.-M. Molina-García-Pardo, J. Pascual-García, and J.-V. Rodríguez, "Experimental study of MIMO-OFDM transmissions at 94 GHz in indoor environments," *IEEE Access*, vol. 5, pp. 7488–7494, 2017.

[9] A. Razavi, A. A. Glazunov, P.-S. Kildal, and J. Yang, "Characterizing polarization-MIMO antennas in random-LOS propagation channels," *IEEE Access*, vol. 4, pp. 10067–10075, 2016.

[10] C. Sacchi, T. Rahman, I. A. Hemadeh, and M. El-Hajjar, "Millimeter-wave transmission for small-cell backhaul in dense urban environment: A solution based on MIMO-OFDM and space-time shift keying (STSK)," *IEEE Access*, vol. 5, pp. 4000–4017, 2017.

[11] G. E. Mueller, "Propagation of 6-millimeter waves," *Proc. IRE*, vol. 34, no. 4, pp. 181p–183p, Apr. 1946.

[12] S. D. Robertson and A. P. King, "The effect of rain upon the propagation of waves in the 1- and 3-centimeter regions," *Proc. IRE*, vol. 34, no. 4, pp. 178p–180p, Apr. 1946.

[13] L. J. Anderson, J. P. Day, C. H. Freres, and A. P. D. Stokes, "Attenuation of 1.25-centimeter radiation through rain," *Proc. IRE*, vol. 35, no. 4, pp. 351–354, Apr. 1947.

[14] R. Wexler and J. Weinstein, "Rainfall intensities and attenuation of centimeter electromagnetic waves," *Proc. IRE*, vol. 36, no. 3, pp. 353–355, Mar. 1948.

[15] T. A. Rahman *et al.*, "Final reports on rain attenuation studies for communication systems operating in tropical regions," Wireless Commun. Centre Res. Lab., Univ. Malaysia, Skudai, Malaysia, Tech. Rep., Oct. 2000.

[16] A. Yagasena and S. I. S. Hassan, "Worst-month rain attenuation statistics for satellite-Earth link design at Ku-band in Malaysia," in *Proc. TENCON*, Sep. 2000, pp. 122–125.

[17] S. C. Sean, J. Din, A. R. Tharek, and M. Z. Abidin, "Studies on characteristics of rain fade at 23 GHz for terrestrial links," in *Proc. Asia–Pacific Conf. Appl. Electromagn. (APACE)*, Aug. 2003, pp. 76–78.

[18] U. Kesavan, M. R. Islam, K. Abdullah, and A. R. Tharek, "Rain attenuation prediction for higher frequencies in microwave communication using frequency scaling technique," in *Proc. Int. Conf. Comput. Commun. Eng. (ICCCE)*, Sep. 2014, pp. 217–219.

[19] M. R. Islam, A. R. Tharek, and J. Chebil, "Comparison between path length reduction factor models based on rain attenuation measurements in Malaysia," in *Proc. Asia–Pacific Microw. Conf.*, Dec. 2000, pp. 1556–1560.

[20] A. Y. Abdulrahman, T. A. Rahman, S. K. A. Rahim, and M. R. U. Islam, "Empirically derived path reduction factor for terrestrial microwave links operating at 15 Ghz in Peninsula Malaysia," *J. Electromagn. Waves Appl.*, vol. 25, no. 1, pp. 23–37, 2011.

[21] K. Ulaganathen, T. A. Rahman, A. Y. Abdulrahman, and S. K. B. A. Rahim, "Comparative studies of the rain attenuation predictions for tropical regions," *Prog. Electromagn. Res. M*, vol. 18, pp. 17–30, Apr. 2011.

[22] S. K. A. Rahim, A. Abdulrahman, T. A. Rahman, and M. U. Islam, "Measurement of wet antenna losses on 26 GHz terrestrial microwave link in Malaysia," *Wireless Pers. Commun.*, vol. 64, no. 2, pp. 225–231, May 2012.

[23] J. Din, "Influence of rain drop size distribution on attenuation at microwave frequency in a tropical region," Ph.D. dissertation, Faculty Elect. Eng., Wireless Commun. Centre, Univ. Technol. Malaysia, Skudai, Malaysia, 1997.

[24] J. Chebil, "Rain rate and rain attenuation distribution for microwave propagation study in Malaysia," Ph.D. dissertation, Faculty Elect. Eng., Univ. Technol. Manage., Shillong, Meghalaya, 1997.

[25] Z. Qingling and J. Li, "Rain attenuation in millimeter wave ranges," in *Proc. 7th Int. Symp. Antennas, Propag. EM Theory (ISAPE)*, Oct. 2006, pp. 1–4.

[26] A. Y. Abdulrahman, T. A. Rahman, S. K. A. Rahim, M. R. Islam, and M. K. A. Abdulrahman, "Rain attenuation predictions on terrestrial radio links: Differential equations approach," *Trans. Emerg. Telecommun. Technol.*, vol. 23, no. 3, pp. 293–301, Apr. 2012.

[27] A. Y. Abdulrahman, T. A. Rahman, S. K. Abdulrahim, and M. R. Islam, "Rain attenuation measurements over terrestrial microwave links operating at 15 GHz in Malaysia," *Int. J. Commun. Syst.*, vol. 25, no. 11, pp. 1479–1488, Nov. 2012.

[28] U. A. Korai, L. Luini, R. Nebuloni, and I. Glesk, "Statistics of attenuation due to rain affecting hybrid FSO/RF link: Application for 5G networks," in *Proc. 11th Eur. Conf. Antennas Propag. (EUCAP)*, Mar. 2017, pp. 1789–1792.

[29] M. C. Kestwal, S. Joshi, and L. S. Garia, "Prediction of rain attenuation and impact of rain in wave propagation at microwave frequency for tropical region (Uttarakhand, India)," *Int. J. Microw. Sci. Technol.*, vol. 2014, Apr. 2014, Art. no. 958498.

[30] O. Fiser, "The role of DSD and radio wave scattering in rain attenuation," in *Geoscience and Remote Sensing New Achievements*. Rijeka, Croatia: InTech, 2010.

[31] M. Marzuki, T. Kozu, T. Shimomai, W. L. Randeu, H. Hashiguchi, and Y. Shibagaki, "Diurnal variation of rain attenuation obtained from measurement of raindrop size distribution in equatorial Indonesia," *IEEE Trans. Antennas Propag.*, vol. 57, no. 4, pp. 1191–1196, Apr. 2009.

[32] L. S. Kumar, Y. H. Lee, and J. T. Ong, "Truncated gamma drop size distribution models for rain attenuation in Singapore," *IEEE Trans. Antennas Propag.*, vol. 58, no. 4, pp. 1325–1335, Apr. 2010.

[33] S. Shrestha and D.-Y. Choi, "Rain attenuation over terrestrial microwave links in South Korea," *IET Microw., Antennas Propag.*, vol. 11, no. 7, pp. 1031–1039, Jun. 2017.

[34] P. Thorvaldsen and I. Henne, "Outdoor transmission measurement at 26 GHz; results of a 4 years trial in prague," in *Proc. 1st URSI Atlantic Radio Sci. Conf. (URSI AT-RASC)*, May 2015, pp. 1–9.
[35] K. Morita, Y. Hosoya, and A. Akeyama, "Some experimental results on 20 GHz band rain attenuation and depolarization," in *Proc. Int. Symp. Antennas Propag. Soc.*, Apr. 1973, pp. 285–288.
[36] P. A. Watson, "Survey of measurements of attenuation by rain and other hydrometeors," *Proc. Inst. Elect. Eng.*, vol. 123, no. 9, pp. 863–871, Sep. 1976.
[37] P. Watson and M. Arbabi, "Rainfall cross-polarization-comparison of theory and measurement," in *Proc. IUCRM Colloq.*, Oct. 1973, pp. I.3-1–I.3-6.
[38] P. Watson and N. McEwan, "Cross polarisation, attenuation and radar reflectivity studies at X-band," ESRO, Paris, France, Tech. Rep. 153, 1974, vol. 2044.
[39] A. Hirata *et al.*, "120-GHz-band wireless link technologies for outdoor 10-Gbit/s data transmission," *IEEE Trans. Microw. Theory Techn.*, vol. 60, no. 3, pp. 881–895, Mar. 2012.
[40] A. Hirata *et al.*, "Effect of rain attenuation for a 10-Gb/s 120-GHz-band millimeter-wave wireless link," *IEEE Trans. Microw. Theory Techn.*, vol. 57, no. 12, pp. 3099–3105, Dec. 2009.
[41] I. Kallfass *et al.*, "64 Gbit/s transmission over 850 m fixed wireless link at 240 GHz carrier frequency," *J. Infr., Millim., Terahertz Waves*, vol. 36, no. 2, pp. 221–233, Feb. 2015.
[42] K. Zheng, L. Zhao, J. Mei, M. Dohler, W. Xiang, and Y. Peng, "10 Gb/s hetsnets with millimeter-wave communications: Access and networking—Challenges and protocols," *IEEE Commun. Mag.*, vol. 53, no. 1, pp. 222–231, Jan. 2015.
[43] *Emerging Trends in 5G/IMT2020*, ITU, Geneva, Switzerland, Sep. 2016. [Online]. Available: https://www.itu.int
[44] D. H. Janzen, "Tropical dry forests," in *Biodiversity*. Washington, DC, USA: National Academies Press, 1988, p. 538.
[45] *Characteristics of Precipitation for Propagation Modelling*, document Rec. P.837-6, ITU-R, P Series, 2013.
[46] *Characteristics of Precipitation for Propagation Modelling*, document Rec. P.7-837, ITU-R, 2017.
[47] M.M. Department. (Jul. 2017). *Monthly Rainfall Review*. [Online]. Available: http://www.met.gov.my/in/web/metmalaysia/climate/climatechange/climateinformation/monthlyrainfallreview
[48] MMD. (Sep. 17, 2017). *Malaysia Meteorology Department*. [Online]. Available: http://www.met.gov.my
[49] T. J. Lutz, "Climatic perception," *J. Geogr.*, vol. 73, no. 9, pp. 21–29, 1974.
[50] K. Robinson, *Where Dwarfs Reign: A Tropical Rain Forest in Puerto Rico*. San Juan, PR, USA: Univ. Puerto Rico, 1997.
[51] C.-P. Chang, Z. Wang, J. McBride, and C.-H. Liu, "Annual cycle of Southeast Asia—Maritime continent rainfall and the asymmetric monsoon transition," *J. Climate*, vol. 18, no. 2, pp. 287–301, 2005.
[52] B. Wang, "Rainy season of the Asian–Pacific summer monsoon," *J. Climate*, vol. 15, no. 4, pp. 386–398, 2002.
[53] P. W. Richards, *The Tropical Rain Forest; an Ecological Study*. Cambridge, U.K.: Cambridge Univ. Press, 1952.
[54] E. Hong, S. Lane, D. Murrell, N. Tarasenko, and C. Christodoulou, "Terrestrial link rain attenuation measurements at 84 GHz," in *Proc. United States Nat. Committee URSI Nat. Radio Sc. Meeting (USNC-URSI NRSM)*, Jan. 2017, pp. 1–2.
[55] J. W. Mink, "Rain-attenuation measurements of millimetre waves over short paths," *Electron. Lett.*, vol. 9, no. 10, pp. 198–199, May 1973. [Online]. Available: http://digital-library.theiet.org/content/journals/10.1049/el_19730145
[56] S. Joshi, S. Sancheti, and A. Goyal, "Rain attenuation measurements for short-range millimetre-wave radio link," *Electron. Lett.*, vol. 42, no. 2, pp. 72–74, Jan. 2006.
[57] M. R. Islam and A. R. Tharek, "Propagation study of microwave signals based on rain attenuation data at 26 GHz and 38 GHz measured in Malaysia," in *Proc. Asia Pacific Microw. Conf.*, vol. 3. Nov./Dec. 1999, pp. 602–605.
[58] L. A. R. Da. Silva Mello, M. S. Pontes, R. M. De Souza, and N. A. P. Garcia, "Prediction of rain attenuation in terrestrial links using full rainfall rate distribution," *Electron. Lett.*, vol. 43, no. 25, pp. 1442–1443, Dec. 2007.
[59] F. C. M. Filho, R. S. Cole, and A. D. Sarma, "Millimetre-wave rain induced attenuation: Theory and experiment," *IEE Proc. H-Microw., Antennas Propag.*, vol. 133, no. 4, pp. 308–314, Aug. 1986.
[60] R. R. persinger, W. L. Stutzman, R. Castle, Jr., and C. W. Bostian, "Millimeter wave attenuation prediction using a piecewise uniform rain rate model," *IEEE Trans. Antennas Propag.*, vol. 28, no. 2, pp. 149–153, Mar. 1980.
[61] J. H. Kim, M.-W. Jung, Y. K. Yoon, and Y. J. Chong, "The measurements of rain attenuation for terrestrial link at millimeter wave," in *Proc. Int. Conf. ICT Convergence (ICTC)*, Oct. 2013, pp. 848–849.
[62] L. D. S. Mello, M. S. Pontes, and E. C. D. Miranda, "Measurements and prediction of outage intensity owing to rain attenuation," *Electron. Lett.*, vol. 48, no. 10, pp. 545–546, May 2012.
[63] S. Ishii, S. Sayama, and T. Kamei, "Measurement of rain attenuation in terahertz wave range," *Wireless Eng. Technol.*, vol. 2, no. 3, pp. 119–124, 2011.
[64] A. Y. Abdulrahman *et al.*, "Investigation of the unified rain attenuation prediction method with data from tropical climates," *IEEE Antennas Wireless Propag. Lett.*, vol. 13, pp. 1108–1111, 2014.
[65] R. M. Islam, Y. A. Abdulrahman, and T. A. Rahman, "An improved ITU-R rain attenuation prediction model over terrestrial microwave links in tropical region," *EURASIP J. Wireless Commun. Netw.*, vol. 2012, no. 1, p. 189, Dec. 2012.
[66] A. Y. Abdulrahman, T. bin Abdulrahman, S. K. bin Abdulrahim, and U. Kesavan, "Comparison of measured rain attenuation and ITU-R predictions on experimental microwave links in Malaysia," *Int. J. Microw. Wireless Technol.*, vol. 3, no. 4, pp. 477–483, 2011.
[67] A. Mauludiyanto, G. Hendrantoro, M. H. Purnomo, T. Ramadhany, and A. Matsushima, "ARIMA modeling of tropical rain attenuation on a short 28-GHz terrestrial link," *IEEE Antennas Wireless Propag. Lett.*, vol. 9, pp. 223–227, 2010.
[68] N. R. Zulkefly, T. A. Rahman, A. M. Al-Samman, A. M. S. Mataria, and C. Y. Leow, "4G channel characterization for indoor environment at 2.6 GHz," in *Proc. IEEE 11th Int. Colloq. Signal Process. Appl. (CSPA)*, Mar. 2015, pp. 63–65.
[69] S. Shrestha and D.-Y. Choi, "Rain attenuation statistics over millimeter wave bands in South Korea," *J. Atmos. Solar-Terrestrial Phys.*, vols. 152–153, pp. 1–10, Jan. 2017.
[70] K. Ulaganathen, M. I. Rafiqul, T. A. Rahman, and M. S. Assis, "Monthly and diurnal variability of rain rate and rain attenuation during the monsoon period in Malaysia," *Radio Eng.*, vol. 23, no. 2, pp. 754–757, 2014.
[71] J. Sander, "Rain attenuation of millimeter waves at λ = 5.77, 3.3, and 2 mm," *IEEE Trans. Antennas Propag.*, vol. 23, no. 2, pp. 213–220, Mar. 1975.
[72] A. Y. Abdulrahman, T. A. Rahman, B. J. Olufeagba, and M. D. R. Islam, "Using full rainfall rate distribution for rain attenuation predictions over terrestrial microwave links in Malaysia," *Signal Process. Res.*, vol. 2, no. 1, pp. 25–28, 2013.
[73] L. Luini and C. Capsoni, "A unified model for the prediction of spatial and temporal rainfall rate statistics," *IEEE Trans. Antennas Propag.*, vol. 61, no. 10, pp. 5249–5254, Oct. 2013.
[74] L. da Silva Mello and M. S. Pontes, "Unified method for the prediction of rain attenuation in satellite and terrestrial links," *J. Microw., Optoelectron. Electromagn. Appl.*, vol. 11, no. 1, pp. 1–14, 2012.
[75] F. J. A. Andrade, Á. A. M. de Medeiros, and L. A. R. da Silva Mello, "Short-term rain attenuation predictor for terrestrial links in tropical area," *IEEE Antennas Wireless Propag. Lett.*, vol. 16, pp. 1325–1328, 2017.
[76] L. Luini and C. Capsoni, "The SC EXCELL model for prediction of rain attenuation on terrestrial radio links," *Electron. Lett.*, vol. 49, no. 4, pp. 307–308, Feb. 2013.
[77] L. Zhao, L. Zhao, Q. Song, C. Zhao, and B. Li, "Rain attenuation prediction models of 60 GHz based on neural network and least squares-support vector machine," in *Proc. 2nd Int. Conf. Commun., Signal Process., Syst.*, 2014, pp. 413–421.
[78] R. Crane, "Prediction of attenuation by rain," *IEEE Trans. Commun.*, vol. 28, no. 9, pp. 1717–1733, Sep. 1980.
[79] R. Ghiani, L. Luini, and A. Fanti, "A physically based rain attenuation model for terrestrial links," *Radio Sci.*, vol. 52, no. 8, pp. 972–980, Aug. 2017.
[80] A. I. Yussuff and N. H. Khamis, "Modified itu-r rain attenuation prediction model for a tropical station," *J. Ind. Intell. Inf.*, vol. 1, no. 3, pp. 155–159, 2013.
[81] F. A. Semire, R. Mohd-Mokhtar, W. Ismail, N. Mohamad, and J. S. Mandeep, "Modeling of rain attenuation and site diversity predictions for tropical regions," *Ann. Geophys.*, vol. 33, no. 3, pp. 321–331, 2015.

[82] D. Das and A. Maitra, "Fade-slope model for rain attenuation prediction in tropical region," *IEEE Geosci. Remote Sens. Lett.*, vol. 13, no. 6, pp. 777–781, Jun. 2016.
[83] F. Moupfouma, "Electromagnetic waves attenuation due to rain: A prediction model for terrestrial or L.O.S SHF and EHF radio communication links," *J. Infr., Millim., Terahertz Waves*, vol. 30, no. 6, pp. 622–632, Jun. 2009.
[84] P. Kántor, J. Bitó, and Á. Drozdy, "Characteristics of 5G wireless millimeter wave propagation: Transformation of rain attenuation applying different prediction models," in *Proc. 10th Eur. Conf. Antennas Propag. (EuCAP)*, Apr. 2016, pp. 1–5.
[85] G. Rakshit, A. Adhikari, and A. Maitra, "Modelling of rain decay parameter for attenuation estimation at a tropical location," *Adv. Space Res.*, vol. 59, no. 12, pp. 2901–2908, Jun. 2017.
[86] J. M. Garcia-Rubia, J. M. Riera, A. Benarroch, and P. Garcia-del-Pino, "Estimation of rain attenuation from experimental drop size distributions," *IEEE Antennas Wireless Propag. Lett.*, vol. 10, pp. 839–842, 2011.
[87] G. Smiatek, F. Keis, C. Chwala, B. Fersch, and H. Kunstmann, "Potential of commercial microwave link network derived rainfall for river runoff simulations," *Environ. Res. Lett.*, vol. 12, no. 3, p. 034026, 2017.
[88] J. C. M. Andersson, P. Berg, J. Hansryd, A. Jacobsson, J. Olsson, and J. Wallin, "Microwave links improve operational rainfall monitoring in Gothenburg, Sweden," in *Proc. CEST*, 2017, pp. 1–4.
[89] D. Caviglia, M. Pastorino, A. Randazzo, and A. Caridi, "A rain estimation system based on electromagnetic propagation models and DVB-S opportunistic sensors," in *Wave Propagation Concepts for Near-Future Telecommunication Systems*. Rijeka, Croatia: InTech, 2017.
[90] M. V. Perić, D. B. Perić, B. M. Todorović, and M. V. Popović, "Dynamic rain attenuation model for millimeter wave network analysis," *IEEE Trans. Wireless Commun.*, vol. 16, no. 1, pp. 441–450, Jan. 2017.
[91] A. A. Harpold *et al.*, "Rain or snow: Hydrologic processes, observations, prediction, and research needs," *Hydrol. Earth Syst. Sci.*, vol. 21, no. 1, pp. 1–22, 2017.
[92] *Propagation Data and Prediction Methods Required for the Design of Earth-Space Telecommunication Systems*, document Rec. ITU-R P.618-12, 2015.
[93] D. Y. Choi, J. Y. Pyun, S. K. Noh, and S. W. Lee, "Comparison of measured rain attenuation in the 12.25 GHz band with predictions by the ITU-R model," *Int. J. Antennas Propag.*, vol. 2012, Jul. 2011, Art. no. 415398.
[94] A. Tokay, P. G. Bashor, E. Habib, and T. Kasparis, "Raindrop size distribution measurements in tropical cyclones," *Monthly Weather Rev.*, vol. 136, no. 5, pp. 1669–1685, 2008.
[95] F. Giannetti *et al.*, "Real-time rain rate evaluation via satellite downlink signal attenuation measurement," *Sensors*, vol. 17, no. 8, p. 1864, 2017.
[96] (2005). *ElvaLink, PPC-1000 Gigabit Ethernet MM-wave Link*. [Online]. Available: http://www.elva-1.com
[97] M. Tamošiunaite, S. Tamošiunas, M. Žilinskas, and M. Tamošiuniene, "Atmospheric attenuation due to humidity," in *Electromagnetic Waves*. Rijeka, Croatia: InTech, 2011.
[98] A. G. Alkholidi and K. S. Altowij, "Free space optical communications—Theory and practices," in *Contemporary Issues in Wireless Communications*. Rijeka, Croatia: InTech, 2014.
[99] *Specific Attenuation Model for Rain for Use in Prediction Methods*, document ITU-R P.838-3, 2005.
[100] J. S. Mandeep, Y. Y. Ng, H. Abdullah, and M. Abdullah, "The study of rain specific attenuation for the prediction of satellite propagation in Malaysia," *J. Infr., Millim., Terahertz Waves*, vol. 31, no. 6, pp. 681–689, Jun. 2010.
[101] H. Y. Lam, L. Luini, J. Din, M. J. Alhilali, S. L. Jong, and F. Cuervo, "Impact of rain attenuation on 5G millimeter wave communication systems in equatorial Malaysia investigated through disdrometer data," in *Proc. 11th Eur. Conf. Antennas Propag. (EUCAP)*, Mar. 2017, pp. 1793–1797.
[102] *Propagation Data and Prediction Methods Required for the Design of Earth-Space Telecommunication Systems*, document Rec. ITU-R P.12-618, 2015, pp. 1–27.
[103] *Propagation Data and Prediction Methods Required for the Design of Terrestrial Line-of-Sight Systems*, document ITU-R P.530-16, 2015.
[104] M. Singh and J. E. Allnutt, "Rain attenuation predictions at Ku-band in South East Asia countries," *Prog. Electromagn. Res.*, vol. 76, pp. 65–74, Sep. 2007.
[105] S. H. Lin, "11-GHz radio: Nationwide long-term rain rate statistics and empirical calculation of 11-GHz microwave rain attenuation," *Bell Labs Tech. J.*, vol. 56, no. 9, pp. 1581–1604, Nov. 1977.
[106] *Propagation Data and Prediction Methods Required for the Design of Terrestrial Line-of-Sight Systems*, document Rec. TU-R P.530-14, 2012.
[107] *The Concept of Worst Month*, document Rec. ITU-R P.581-2, 2001, p. 1.
[108] *Conversion of Annual Statistics to Worst-Month Statistics*, document ITU-R P.841-5, ITU, 2016.
[109] K. Ulaganathen, T. A. Rahman, S. K. A. Rahim, and R. M. Islam, "Review of rain attenuation studies in tropical and equatorial regions in Malaysia: An overview," *IEEE Antennas Propag. Mag.*, vol. 55, no. 1, pp. 103–113, Feb. 2013.
[110] J. Chebil and T. A. Rahman, "Worst-month rain statistics for radiowave propagation study in Malaysia," *Electron. Lett.*, vol. 35, no. 17, pp. 1447–1449, Aug. 1999.
[111] WCC, "Final reports on rain attenuation studies for communication systems operating in tropical regions," Wireless Commun. Centre, Univ. Teknologi Malaysia, Skudai, Malaysia, Tech. Rep., Oct. 2000.
[112] M. Juy, R. Maurel, and M. Rooryck, "Monthly distribution of rain rate and attenuation measured in Indonesia," in *Proc. URSl Commission F Open Symp. Regional Factors Predicting Radio Wave Attenuation Due Rain*, 1990, pp. 155–159.
[113] A. Yagasena, S. I. S. Hassan, and M. M. M. Yusoff, "Rain attenuation prediction at 6.75 GHz in Malaysia using rain gauge and radiometer measurements," in *Proc. IEEE Singapore Int. Netw., Theme, Electrotechnol., Commun. Netw. Int. Conf. Inf. Eng.*, Jul. 1995, pp. 596–599.
[114] R. K. Crane, *Propagation Handbook for Wireless Communication System Design*. Boca Raton, FL, USA: CRC Press, 2003.
[115] Google. *Internet Resources Dated*. [Online]. Available: http://www.googlemap.com
[116] ATDI. (May 2017). *ATDI ICS Telecom EV*. [Online]. Available: http://www.atdi.com/ics-telecom/
[117] NASA. *The Shape of a Raindrop*. [Online]. Available: https://pmm.nasa.gov/education/articles/shape-of-a-raindrop
[118] M.M. Department. (1987). *Annual Reports of 1987*. [Online]. Available: http://www.met.gov.my
[119] E. Casiraghi and A. Paraboni, "Assessment of CCIR worst-month prediction method for rain attenuation," *Electron. Lett.*, vol. 25, no. 1, pp. 82–83, Jan. 1989.

IBRAHEEM SHAYEA received the B.Sc. degree in electronic engineering from the University of Diyala, Iraq, in 2004, the M.Sc. degree in computer and communication engineering and the Ph.D. degree in mobile communication engineering from the Universiti Kebangsaan Malaysia, Malaysia, in 2010 and 2015, respectively. He is currently a Researcher with the Wireless Communication Centre, Universiti Teknologi Malaysia (UTM), Kuala Lumpur, Malaysia, and also a Researcher with the Wireless Communication Centre. He has published over eight papers related to wireless communication in national/international journal and conference. His research interests are mobility management, handover, LTE/LTE-A, carrier aggregation, radio propagation, and indoors and outdoors wireless communication.

THAREK ABD. RAHMAN received the B.Sc. degree in electrical and electronic engineering from the University of Strathclyde, U.K., in 1979, the M.Sc. degree in communication engineering from the University of Manchester Institute of Science and Technology, Manchester, U.K., and the Ph.D. degree in mobile radio communication engineering from the University of Bristol, U.K., in 1988. He is currently a Professor with the Faculty of Electrical Engineering, Universiti Teknologi Malaysia, and also the Director of the Wireless Communication Centre. His research interests are radio propagation, antenna and RF design, and indoors and outdoors wireless communication. He has been conducted various short courses related to mobile and satellite communication to the Telecommunication Industry and Government body since 1990. He has a teaching experience in the area of mobile radio, wireless communication system, and satellite communication. He has published over 120 papers related to wireless communication in national/international journals and conferences.

MARWAN HADRI AZMI received the B.Eng. degree (Hons.) in electrical and telecommunications from the Universiti Teknologi Malaysia (UTM) in 2003, the M.Sc. degree in communications and signal processing from the Imperial College of Science, Technology and Medicine, University of London, in 2005, and the Ph.D. degree from the University of New South Wales, Australia, in 2012. From 2012 to 2014, he spent his Sabbatical leave of absence with McGill University, Canada, involved in the funded project by RIM Inc. and NSERC, entitled Cooperative Spectrum Sensing and Information Relaying in Cognitive Wireless Communications. He is currently a Senior Lecturer with the Wireless Communication Centre, UTM. His research interests include mobile and wireless communications, communication theory, error control coding, relay networks, spectrum sensing for cognitive radio, and iterative receiver.

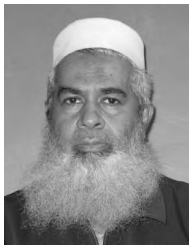

MD. RAFIQUL ISLAM received the B.Sc. degree in electrical and electronic engineering from the Bangladesh University of Engineering and Technology, Dhaka, and the master's degree in electrical engineering, the Ph.D. degree in electrical engineering, and the Ph.D. degree from Universiti Teknologi Malaysia. He is currently a Professor with the Faculty of Electrical Engineering, International Islamic University Malaysia. He was a leader for several research projects and he also involved in various research projects in wireless communication. He also has a good teaching experience in the area of mobile radio communication, wireless communication system, and antennas. He has published several review and research papers in national/international journals and conferences. His research interests are in radio link design, RF propagation measurement and RF design, smart antennas, and array antennas design.